# Testing the application of novel technology for monitoring grape vine health and berry maturity using transmitted visible and near infrared light

by

Bronwyn Riddoch

A thesis

presented to the University of Waterloo

in fulfillment of the

thesis requirement for the degree of

Master of Science

in

Geography

Waterloo, Ontario, Canada, 2025

## Author’s Declaration

I hereby declare that I am the sole author of this thesis. This is a true copy of the thesis, including any required final revisions, as accepted by my examiners.

I understand that my thesis may be made electronically available to the public.

## Abstract

Climate change is impacting wine-growing regions globally, with varying effects on vineyards. While some regions may benefit from warmer temperatures, others may face detrimental consequences, especially with the predicted increase in extreme weather events or less than optimal conditions. Precision viticulture uses remote and proximal sensing technologies to monitor these changes and adapt vineyards by providing insights into vine health and grape maturity. This information can be used to determine when intervention is needed in vineyards to maintain grape quality. However, existing precision viticulture methods are limited, such as the inability to provide continuous, real-time data and the utilization of reflected light, which can lead to inaccurate measurements. Current research has not yet investigated the potential of using transmitted light for monitoring vine health and grape maturity, a method that could provide more accurate insights. This thesis seeks to fill this gap by evaluating the feasibility of applying a novel system, TreeTalker-Wine© (TTW), to continuously monitor grapevine health and maturity through transmitted light in commercial vineyards.

To test the application of TTWs for monitoring vine health, the sensors were deployed under the canopy of Cabernet Franc in two commercial vineyards in Niagara, Ontario, Canada. Spectral data collected by the TTWs was used to calculate the daily Normalized Difference Vegetation Index ($NDVI_T$) based on transmitted light. The resulting $NDVI_T$ values were consistent with expected ranges and aligned with viticultural management practices and weather events. To assess the potential of TTWs for monitoring grape maturity, partial least squares (PLS) models were developed for Cabernet Franc, Chardonnay, and Riesling varieties using

spectral data from the grape clusters, along with air temperature and Total Soluble Solids (TSS) content. Grape clusters were collected bi-weekly from a third vineyard in Niagara, Ontario, Canada, starting at the pea-size stage and continuing through veraison. After veraison, sampling frequency increased to weekly until harvest. After each collection day, the fruit was transported to a laboratory with a plant growth chamber designed to replicate the vineyard's environmental conditions. Grape clusters were suspended over the TTWs in the plant growth chamber to collect spectral signatures of the fruit before the entire cluster was juiced to determine TSS content. The results of the PLS models suggest that TTWs are able to determine TSS content from the spectral signatures of the grape clusters, however unique models are required for each grape variety. These findings indicate that TTWs offer a promising approach to precision viticulture. Future research is needed to assess a broader range of grape varieties to better understand the relationship between $NDVI_T$ and vine health, as well as to refine the TSS prediction models. This will enable further exploration of the potential of transmitted light in monitoring grapevine health and maturity, supporting more accurate and timely viticulture practices in changing climate.

## Acknowledgements

There are countless individuals who have supported me in the creation of this thesis, offering their time, knowledge, and encouragement throughout this journey. I am deeply grateful to each and every one of you.

Thank you to my supervisor, Dr. Richard Petrone, for giving me the opportunity to join the Vineyard Project within the Hydrometeorological Group. I am grateful for your guidance and support over the past two years and for allowing me to work on a research project that aligns with my diverse interests.

Thank you to Dr. Myroslava Khomik for your invaluable assistance in the field and for your continued mentorship and encouragement. Your expertise and advice have been instrumental throughout this process.

A heartfelt thank you to Jessica Williamson, Eric Murray, and everyone in the Hydrometeorological Group for your technological support and for sharing your knowledge.

Thank you to Rosewood Estates Winery and Thirty Bench Wine Makers for graciously allowing me to conduct my research in your beautiful vineyards. A special thank you to Doug Mackenzie for providing me with lab space at Rosewood and for patiently answering my many questions.

To Maia Moore, thank you for your unwavering friendship and for being my sounding board throughout this journey. And to the rest of the Haddon House—Anna, Grace, Mya, and Shannon—thank you for your friendship and support.

Lastly, to my parents, Ashley and Andrea Riddoch—this thesis is possible because of you. Thank you for your unconditional love, patience, and support. I couldn't have done it without you. Thank you.

# Table of Contents

## List of Figures

## List of Tables

# Chapter 1: Introduction and Literature Review

## 1.1 Introduction

To ensure the highest quality wine, viticulturists closely monitor the health and productivity of grapevines (*Vitis vinifera CV*), as berry quality directly impacts wine quality (Hall et al., 2002). The health and productivity of grapevines are influenced by a number of factors, including climatic conditions and the physical and chemical characteristics of vineyard soils (Gutiérrez-Gamboa et al., 2021; Van Leeuwen and Seguin, 2006). Additionally, the high heterogeneity in vineyard structure—often characterized by trellised grapevines, interrow cover crops, and bare soil—results in increased spatial variability, leading to different physiological responses in vines across the vineyard (Gatti et al., 2022; Yu et al., 2020).

It is essential for viticulturists to use efficient sampling methods to assess this variability, enabling them to adapt vineyard management practices based on vine responses. Traditional vineyard monitoring methods, while essential, tend to be destructive, labor-intensive, time-consuming and rely on manual and random sampling of berries and vines within a block (Oliveira et al., 2024). For instance, water stress in vines, which helps determine whether irrigation is necessary, is typically measured using a pressure chamber in the field. This method requires the collection of leaves from multiple vines and is time intensive to obtain readings that accurately represents the spatial variability of water stress in the vineyard (Kotsaki et al., 2020a, 2020b; Reynolds et al., 2018; Romero et al., 2018). Similarly, monitoring grape maturity to determine optimal harvest time traditionally involves harvesting grape samples, juicing the fruit and then measuring the must (grape juice prior to fermentation) in a refractometer, either in the field or laboratory. However, this method is also destructive and time-consuming and must be performed several times a growing season to understand how the grape is developing (Kasimati et al., 2022;

Urraca et al., 2016). Additionally, these methods provide a discreet dataset, making it difficult for viticulturists to understand the spatial variability of the vineyard.

The wine industry, like many others, faces the challenges posed by anthropogenic climate change. Climate variability has already started to threaten the stability of wine production, particularly in traditional viticulture regions. Warming trends during the growing season have been observed across key viticulture regions (Molitor and Junk, 2019; Santos et al., 2020). While some regions, such as Central and Northern Europe, may be able to cope with these shifts in climate by adapting vineyard management practices, others, like Southern Europe, are predicted to become unsuitable for wine production altogether (Droulia and Charalampopoulos, 2021). In Napa, California—a major wine-producing region—drastic temperature increases are forcing grape growers to adapt their practices to maintain wine quality (Gambetta and Kurtural, 2021). Similarly, Ontario growing season temperatures are also warming, with regions like the Niagara Peninsula and Lake Erie North Shore transitioning from cool to intermediate climate zones, initiating change to the standard vineyard management practice in the region (Shaw, 2017; Hewer and Brunette, 2020).

In light of these challenges, the continued reliance on traditional vineyard monitoring methods limits the ability of viticulturists to respond and adapt effectively to changing climatic conditions in the vineyards. Traditional methods lack the flexibility and scalability required to optimize vineyard performance in the face of climate change (Gutiérrez et al., 2019). In contrast, the application of precision viticulture—an innovative approach that leverages technology—can help viticulturists monitor vineyard responses to climate variability, enabling real-time decision-making during the growing season (Matese and Gennaro, 2015). Precision viticulture allows viticulturists to collect data on vine health and productivity at high spatial resolution using non-

destructive, efficient techniques, which provide a more robust application for adapting vineyard management practices in the future.

## 1.2 Literature Review

### 1.2.1 Vineyard Vulnerabilities to Climate Change

The impact of changing temperatures on grape maturation is a critical concern for viticulture, as fluctuations in temperature during key stages of grape development can significantly affect wine quality. When temperatures change as the grape is maturing there can be significant impact to wine quality (van Leeuwen et al., 2024). Periods of sustained high summer temperatures can produce grapes with higher sugar content and lower pH, resulting in wines with high alcohol levels, and a cooked fruit aroma, compared to the desirable fresh fruit aromas (Fraga, 2019; Pons et al., 2017). Alternatively, depending on the timing of the extreme heat event, the sugar accumulation and metabolic processes in the vines may come to a halt, resulting in unripe grapes and wines that tend to have a green and acidic profile (Pickering et al., 2015a; Pons et al., 2017). Furthermore, if extreme heat occurs near harvest, it may decouple the accumulation of sugars and anthocyanins in the fruit, making it more challenging to determine the optimal harvest time to capture the best grape profile (Sadras and Moran, 2012; van Leeuwen et al., 2024).

Water stress to the vines can also have a significant impact on wine quality. During periods of drought, if the vines undergo major water stress, the berry size and quantity of juice will be reduced and shoot development will be slowed, particular if drought occurs before veraison (Ojeda et al., 2001; Pickering et al., 2015b). However, if vines only experience mild water stress, it has been shown that the grapes will have a higher phenolic concetration, which is a diserable characteristic for producing a high quailty wine (Espinoza et al., 2017; van Leeuwen et al., 2024). On the contrary, if there are extreme rainfall events, sugar content, acidity and pigment synthesis

are commonly negatively affected decreasing wine quality, but there would be an increase of vegetative growth and yield (Pickering et al., 2015a).

Another concern for wine quality in vineyards affected by climate change is the development of more favorable conditions for pests, diseases, and numerous invasive species that prey on grapevines (van Leeuwen et al., 2024). One such invasive species, *Spotted Wing Drosophila* (SWD), is expected to expand its range with warmer temperatures, putting more vineyards at risk (van Leeuwen et al., 2024). The female SWDs lay their eggs in the fruit prior to harvest, and the larvae that develop inside cause the berries to decay more quickly than unaffected fruit, leading to reduced crop size and potential quality losses (Lee et al., 2011). In addition to pests, fungal diseases like downy and powdery mildew, the greatest fungal threat in vineyards, are expected to become more common with a changing climate (Gessler et al., 2011; Rienth et al., 2021; van Leeuwen et al., 2024). Specifically in regions where more extreme precipitation events occur, downy mildew is predicted to become much more common due to the pathogens preference for moist environments (Gessler et al., 2011; van Leeuwen et al., 2024). Foliar infections of mildew can lead to the losses of photosynthetic leaf area, resulting in lower berry sugar content and decreased berry yield (Rienth et al., 2021).

In addition to concerns during the growing season, climate change also poses several risks to vine health during the dormmate phase as well. Budbreak has been occurring earlier in many regions; however, the increasing unpredictability of weather events exposes vines to a higher risk of frost damage in the spring (Sgubin et al., 2018; van Leeuwen et al., 2024). While the trend of warming winters in some regions has overall resulted in less winter vine damage, other regions are experiencing climatic changes that put vines at greater risk of winter damage. For example, short periods of more extreme winter temperatures increases winter damage, which can have profound

impacts on next seasons grape yield (Shaw, 2017). Similarly, a reduction in cold hardening due to more mild fall temperatures, an increase in the frequency of winter freeze-thaw events, and a decrease in protective snow cover can result in increased winter damage (Fund et al., 2001).

The primary vulnerabilities within vineyards under changing climate center around (i) maintaining vine health and (ii) determining the optimal fruit harvest time. As extreme weather events become more common, management practices will require adaptation to ensure that the vines can withstand extreme heat and cold, excessive water and drought, and an increase in disease pressures that changing climate presents (Fund et al., 2001; Gessler et al., 2011; Shaw, 2017; Rienth et al., 2021; Sgubin et al., 2018; van Leeuwen et al., 2024). Additionally, adaptations to the standard berry monitoring procedures will become a necessity to facilitate a comprehensive understanding of the fruit quality, as the timing of grape maturation varies due to an increase of weather events, such has extreme heat and significant precipitation, influencing the metabolic processes of maturation (Espinoza et al., 2017; Ojeda et al., 2001; Pickering et al., 2015a; Pickering et al., 2015b; Pons et al., 2017; Sadras and Moran, 2012; van Leeuwen et al., 2024). The potential ramifications of climate change to viticulture underscores the need for the development and implementation of technology which can aid in the continuous monitoring of vineyards to help support adaptation of grape production in changing climate.

### 1.2.2 Precision Viticulture for Enhanced Vine Health Monitoring

Solar radiation is reflected, absorbed, and transmitted through the leaves of the vine canopy (Chowdhury et al., 2024). Each pigment of the leaf has a specific spectral absorption pattern, and by quantifying how the light interacts, insight can be derived into the overall health of the vine (Chowdhury et al., 2024; Zahir et al., 2022). For example, leaves of healthy vines absorb in the red (620–780 nm) and blue regions (440–490 nm), due to the high chlorophyll content (Liew et

al., 2008; Zahir et al., 2022). Spectrometers are a tool that can be implemented to quantify how the light specifically interacts with the leaves and allows for non-destructive insight into overall plant health by measuring how much of each band length is reflected or transmitted through the leaves (Chowdhury et al., 2024).

Vegetation indices (VIs) use known mathematical relationships between specific spectral radiation bands, collected by spectrometers, to quantify reflected light interactions with the vegetation canopy (Chowdhury et al., 2024; Matese and Gennaro, 2015). The most well-known VI is the normalized difference vegetation index (NDVI), which was first introduced in 1973 (Giovos et al., 2021; Matese and Gennaro, 2015). NDVI uses the red and near infrared bands to allow for the quantification of chlorophyl content in plants and is commonly used in most agricultural settings. As many of the impending threats of climate change in vineyards, impact the photosynthetic capacity of the vines, and therefore the chlorophyll content of the vine, NDVI is an important metric to monitor in vineyards. In a vineyard setting, NDVI assesses the photosynthetic function of the vines, and therefore, can be utilized to identify when intervention with pesticides and irrigation can help preserve berry quality (Chowdhury et al., 2024; Mucalo et al., 2024; Serrano and Gorchs, 2022).

Remote sensing, one of the techniques used with precision viticulture which utilizes spectrometers, can rapidly provide an assessment of vineyard health using NDVI (Matese and Gennaro, 2015). Two commonly used remote sensing methods are satellites and unmanned aerial vehicles (UAVs). Within agricultural, satellites are typically used to provide the data needed to calculate VIs and allow for insight to be gained but they are not typically suitable for viticultural because higher resolutions are needed to distinguish the high heterogeneity in vineyards (Matese

and Gennaro, 2015). UAVs are the preferred method for collecting data in viticulture due to the higher spatial resolution that can be collected (Matese and Gennaro, 2015).

NDVI calculated with remote sensing methods has been shown to be linearly related to canopy growth, and canopy growth has been shown to be a key factor in determining grape vine water use. Therefore, water status of the vines can be related to NDVI through linear regression (Diago et al., 2022). Serrano et al. (2012) identified a relationship between water availability and NDVI in Chardonnay grapes. In Niagara, low NDVI zones correspond to low leaf water potential, meaning that the vines are experiencing high water deficits (Reynolds et al., 2018) . However, it has also been suggested that NDVI may only be able to accurately predict water stress 40 days or less before harvest (Espinoza et al., 2017).

NDVI can also be used to understand Leaf Area Index (LAI) in vineyards. NDVI captures the temporal differences of LAI in vineyards and has been shown to be linearly correlated (Johnsonet al., 2001; Johnson et al., 2003). Fuentes et al. (2014) verified more recently that NDVI and LAI are strongly correlated. NDVI data collected in vineyards for LAI prediction is temporally stable for three to five years at a time in mature vines, which can help support grape producers when making decisions for subsequent years (Kazmierski et al., 2011).

Using NDVI to predict vine vigour is not without its challenges. Although NDVI is known to be a strong indicator of vigour in agriculture, a crop such as vines poses challenges due to the discontinuous nature of the ground cover (Fuentes et al., 2014; Khaliq et al., 2019; Matese and Di Gennaro, 2021). Additionally, NDVI might not be able to predict LAI in all vineyard settings. Johnson (2003) found that NDVI tends to saturate at higher LAIs, so using NDVI to predict LAI may not be as accurate in minimally pruned sites. However, Khaliq et al. (2019) found that using

UAV data as opposed to satellite derived data increased the correlation of NDVI to LAI, suggesting that using UAV to remote sense in this case may be the most accurate.

Proximal sensing is another measuring technique that allows for knowledge of spatial and temporal variability in vineyards by using ground-based techniques (Matese and Gennaro, 2015). The data is typically collected with a vehicle on the ground, outfitted with sensors, that drives through the rows of vineyards (Gatti et al., 2016). Of additional benefit, proximal sensed data tends to be of a higher quality than remotely sensed data and can be collected with very little effort (Ammoniaci et al., 2021). Some of the commercially available proximal sensors include MECS-VINE®, GreenSeeker, and CropCircle (Gatti et al., 2016; Reynolds et al., 2018; Kotsaki et al., 2020a; Ammoniaci et al., 2021; Kasimati et al., 2022). All of which have been shown to have a high correlation to UAV and satellite-derived data (Gatti et al., 2016; Reynolds et al., 2018; Ammoniaci et al., 2021; Squeri et al., 2021; Kasimati et al., 2022). However, these proximal sensors are still limited as they are required be mounted to a vehicle such as a tractor to collect data throughout the vineyards, therefore not offering continuous data collection (Gatti et al., 2016; Reynolds et al., 2018; Ammoniaci et al., 2021; Kasimati et al., 2022).

While NDVI and other VIs offer valuable insights into vineyard health and performance using remote and proximal sensing techniques, challenges such as high vegetation density and mixed pixel issues highlight the need for continued innovation in sensing technology to optimize vineyard management and better predict the impacts of climate change on vine productivity.

### 1.2.3 Precision Techniques for Non-Destructive Grape Monitoring

Grapes used in wine production are carefully monitored throughout their development, particularly as they approach maturity, because grape composition at harvest is a key determinant of wine quality. One of the most critical factors influencing wine quality is the sugar content,

measured as Total Soluble Solids (TSS), of the grape at the time of harvest (Jordão et al., 2015; Sinton et al., 1978). High sugar content in grapes is a desirable trait, as the sugar is converted into alcohol during fermentation, transforming grape must into wine (Conde et al., 2007; Jordão et al., 2015). Therefore, sugar content is one of the primary indicators used to determine the optimal harvest time (Conde et al., 2007). However, the rate at which sugar accumulates in grape berries is not always predictable, as it is closely tied to the weather conditions impacting the vineyard (Jackson and Lombard, 1993).

Near-Infrared (NIR) analysis is a powerful, non-destructive tool widely used for estimating TSS content in fruits, including grapes (Dambergs et al., 2015; Fernández-Novales et al., 2019a; Nicolaï et al., 2007). This technique measures the interaction of electromagnetic radiation in the 780–2500 nm range with the fruit's chemical components. The specific wavelengths absorbed by these components provide valuable information about the fruit’s composition (Nicolaï et al., 2007).

NIR spectroscopy is particularly effective for grape maturity estimation because the NIR region interacts with molecular overtones and combination bands of chemical bonds, such as O-H, C-H, and N-H (McGlone and Kawano, 1998; Dambergs et al., 2015; Pu et al., 2016; Chandrasekaran et al., 2019; Fernández-Novales et al., 2019a). These bonds are prevalent in sugars and water, the primary components contributing to TSS. By analyzing the absorption patterns and intensities of the NIR light range, predictive models can be developed to estimate TSS accurately and efficiently (Chandrasekaran et al., 2019).

Many past studies on fruits such as melons, kiwifruit, pomegranates and grapes have demonstrated the successful use of NIR spectroscopy in laboratory settings to predict fruit ripeness (Giovenzana et al., 2014; Khodabakhshian et al., 2017; Pampuri et al., 2022; Walsh et al., 2020; Wang and Paliwal, 2007; Yang et al., 2019). However, these studies were often conducted under

controlled conditions, such as stable illumination, temperature, and humidity, which limits the transferability of spectral relationships in field settings where environmental variables are difficult to control (Gutiérrez et al., 2019). Although NIR spectroscopy has been successfully applied to grape maturity prediction in the vineyard (Herrera et al., 2003; Larrain et al., 2008; Urraca et al., 2016), its practical use remains limited. The method's ability to focus on only small areas of the grapevine means that individual berries must be accessed, which restricts the amount of data that can be collected during field assessments (Gutiérrez et al., 2019).

Hyperspectral imaging offers an alternative to traditional NIR spectroscopy. While both techniques rely on similar principles of light-fruit interaction to analyze molecular bonds, hyperspectral imaging is more suited for field applications. It can capture data across a broader spectrum and from larger areas simultaneously, allowing for the analysis of multiple wavelengths at once (Gutiérrez et al., 2019). Additionally, hyperspectral cameras can be easily mounted on field equipment to collect large datasets with minimal environmental influence (Chandrasekaran et al., 2019; Gutiérrez et al., 2019).

Gutiérrez et al. (2019) conducted one of the first studies to use hyperspectral imaging for predicting grape maturity, focusing on Tempranillo grapes (a red variety) in Spain. In their approach, a hyperspectral camera was mounted on an all-terrain vehicle, which was driven through the vineyard to collect spectral data. The resulting model was highly successful in predicting TSS, achieving a high coefficient of determination ($R^2 = 0.92$) (Gutiérrez et al., 2019). This demonstrated the potential of hyperspectral imaging for large-scale, non-destructive grape maturity monitoring in vineyard settings.

Similarly, Benelli et al. (2021) utilized a hyperspectral camera mounted on a garden cart to scan a row of Sangiovese grapes in a vineyard in Italy. The data collected in the 400–1000 nm

spectral range was also used to model TSS, achieving a strong prediction ($R^2 = 0.81$). Notably, Benelli et al. (2021) suggested that the NIR range (700–1000 nm) was particularly critical for TSS prediction, proposing that excluding the visible spectrum (400–700 nm) could simplify future models without sacrificing accuracy.

Despite the promising results, both studies identified several practical challenges in implementing hyperspectral imaging for vineyard management. Gutiérrez et al. (2019) encountered issues related to irregular terrain, vehicle vibrations, and variable speed, which affected the consistency of the data collection. They noted that these factors should be addressed in future studies to improve the reliability of hyperspectral imaging systems in field conditions.

Benelli et al. (2021) also faced challenges related to environmental factors. The need for frequent calibration of the camera was highlighted, as varying light conditions due to cloud cover could introduce errors into the spectral data. Additionally, both studies observed that the presence of excess foliage could obscure the fruit and degrade the quality of the spectral readings (Gutiérrez et al., 2019; Benelli et al., 2021). To mitigate this, Benelli et al. (2021) suggested that additional leaves above normal vineyard management practices may need to be removed to ensure clearer fruit measurements.

Remote sensing techniques, particularly those using NDVI data, are also widely used for predicting grape maturity. High NDVI data from UAVs has been linked to high levels of TSS later in the growing season (Kasimati et al., 2021; Reynolds et al., 2018), though the strength of this relationship increases in the latter half of the growing season (Fredes et al., 2021; Kasimati et al., 2021). While NDVI is often used, alternative VIs, such as the Transformed Chlorophyll Absorption in Reflectance Index/Optimal Soil Adjusted Vegetation Index (TCARI/OSAVI), have also shown promise in estimating TSS (Soubry et al., 2017). Some of the variability seen in NDVI

and TSS relationships are accounted for in varietal differences. Riesling has been shown to have an inverse relationship of TSS to NDVI; whereas Cabernet frac NDVI was shown to be positively correlated to TSS (Kotsaki et al., 2020a).

Although UAV data is preferred for estimating TSS due to its higher spatial resolution, satellites like Sentinel-2 (S2) can also be used. Incorporating additional bands, such as B11 and B12 (short-wave infrared), into NDVI models significantly improves the correlation with Brix estimates (Fredes et al., 2021). However, models based on S2 NDVI data show weaker correlations than those based on UAV data, indicating that UAVs are more suitable for accurate Brix prediction (Kasimati et al., 2022).

Remote sensing technologies and NIR analysis, offer valuable insights into grape maturity and TSS prediction. However, challenges related to environmental factors and data consistency must be addressed to improve the accuracy and practical application of these tools in vineyard management to help navigate climate change.

### 1.3 Research Gaps

The literature has demonstrated that climate change is affecting all wine-growing regions globally. While the impacts of climate change will vary by region, the specific effects of climate change on individual vineyards remain uncertain. Some wine regions may benefit from warmer temperatures, while others may experience detrimental effects. One climate change impact highlighted in the literature is the expected increase in extreme weather, which will have significant consequences for grape characteristics and, consequently, wine quality (Pickering et al., 2015a; Shaw, 2017). As a result, precision viticulture is seen as a promising tool to help monitor and adapt vineyards to the changing climate, enabling vintners to better understand the effects of climate change on grape health.

Significant research has been conducted on how to effectively implement precision viticulture. Remote and proximal sensing technologies have been extensively explored for monitoring vine health in vineyards. UAVs typically outperform satellites in vineyard settings. However, due to the space between vineyard rows, remote sensing techniques sometimes struggle to differentiate between vines and ground cover, leading to a mix-pixel effect. Proximal sensing has been shown to alleviate this issue, improving the accuracy of predictions regarding vine health and grape maturity. NDVI calculated from both remote and proximal sensing, is a versatile VI that has shown strong correlations with TSS, vine water stress, and vigor. However, one major drawback of using NDVI in these methods is the risk of saturation in areas with high LAI which can limit the sensitivity of the measurements.

While remote and proximal sensing methods are useful for monitoring grape maturity, they often rely on vine health as a proxy, leaving much uncertainty regarding the direct factors that influence TSS development in grapes (Soubry et al., 2017; Matese et al., 2022). NIR spectroscopy has been used to assess fruit ripeness in a laboratory setting, but its field application is limited due to uncontrollable environmental factors and the fact that it only produces a discrete dataset. In contrast, hyperspectral imaging is being explored to generate continuous datasets for monitoring grape maturity.

Recent studies have shown that hyperspectral imaging can produce highly accurate models for grape maturity. Benelli et al. (2021) suggest that focusing on the NIR portion of the electromagnetic spectrum is particularly important for modeling grape maturity, as these wavelengths correlate strongly with grape composition. Despite the promising results, such as the need for precise calibration in varying light conditions limits the application of this technology in vineyards (Benelli et al., 2021).

While there have been significant advancements in remote and proximal sensing technologies for monitoring vine health in response to climate change, current methods still have limitations. None of the existing techniques allow for continuous, real-time monitoring of vineyards. All current methods are dependent on satellite flyovers, UAV flights, or vehicle drives to collect data, which are inherently limited by timing, coverage, and environmental conditions. Furthermore, the majority of monitoring techniques focus on reflected light, often overlooking the potential of transmitted light through the vine canopy, which could provide additional valuable insights to both vine health and grape quality.

Traditional NDVI calculations are based on the principle that red wavelengths are absorbed by chlorophyll pigments, while NIR wavelengths are reflected due to the absence of NIR-absorbing compounds in leaf structures (Knipling, 1970; Rous et al., 1973; Woolley, 1971). However, studies by Knipling (1970) and Woolley (1971) show that NIR wavelengths are both reflected and transmitted through leaves in nearly equal proportions. This suggests that NDVI can be adapted to monitor canopy health using transmitted light. As previously discussed, traditional NDVI methods, which capture reflected light, may include information from areas outside the canopy of interest, such as ground cover (Matese and Gennaro, 2015), resulting in mixed pixels. In contrast, capturing light transmitted through the canopy would allow for more focused monitoring of the canopy itself. Additionally, the use of transmitted light to monitor grape maturity has been suggested to be more accurate than reflective methods as the light must pass through the fruit sample and therefore can provide valuable information about the internal conditions of the sample (Chandrasekaran et al., 2019). However, the NIR analysis methods used for determining TSS of the grape in a vineyard setting still focus on the use of reflected light (Benelli et al., 2021; Ebrahimi et al., 2024; Gutiérrez et al., 2019). The application utilizing transmitted light for crop

monitoring is an aspect that has not been fully explored in the context of grapevine health and maturity, presenting an area for future research.

Given precision viticulture technology still does not allow for the real-time, continuous monitoring of vine health and grape maturity throughout the growing season, and does not use transmitted light, the ability to employ transmitted light in a continuous monitoring system has the potential to improve viticulture management. One promising technology that could address this gap is TreeTalker© (TT), a novel system being developed for monitoring forest health through transmitted light. TTs use spectral sensors to measure light transmitted through the canopy, offering a unique perspective compared to traditional satellite or UAV-based methods, which measure reflected light from above. TTs can be deployed to continuously gather data on forest health, transmitting this information through the Internet of Things (IoT) to computer servers for real-time analysis (Vaglio Laurin et al., 2024; Valentini et al., 2019). In preliminary studies, TTs with sensors positioned upwards to measure transmitted light, have been shown to avoid interference from understory vegetation, providing a clearer view of canopy changes (Vaglio Laurin et al., 2024). Additionally, TTs can offer a more complete data set, free from the gaps that typically occur in satellite data due to cloud cover or flyover timing.

Building on its success in forest health monitoring, TT technology has the potential to be adapted for vineyards, creating a TreeTalker-Wine© (TTW) system. This system could enable continuous monitoring of grapevine health and maturity through transmitted light measurements, filling a critical gap in precision viticulture. By providing real-time data on grapevine responses to changing climate conditions, TTWs could help viticulturists make more informed decisions to optimize vine health and grape quality.

## 1.4 Research objectives

The objectives of this thesis are to: (i) evaluate the feasibility of utilizing the TTW system to provide continuous monitoring of *V. vinifera cv.* health in a commercial vineyard setting; (ii) determine if the TTW spectrometer can collect spectral information on the light transmitted through the vineyard canopy in multiple band lengths, from which NDVI can be derived to monitor vine health; and (iii) investigate the potential of using TTWs for monitoring grape cluster maturity for optimal harvest timing.

# Chapter 2: Methods

## 2.1 Tree Talker Wine Sensor

The TTW system utilizes IoT technology for near-real-time monitoring of grapevine health, adapted from the original TT system, which was designed for monitoring trees in forests. The TTW system specifically focuses on vineyards, with each sensor, housed in a compact 11.5 x 6.5 x 6 cm plastic case. Inside the casing, an ATMega 328 processor collects data on key viticultural factors, including light transmission through the canopy or fruit, sap flow in the vine's trunk, soil temperature and moisture, and air temperature and relative humidity. Each TTW is powered by a 3.7V lithium-ion battery and a small solar panel attached to the battery case. Although not utilized in this study, the TTW system can wirelessly transmit the collected data from each TTW to a TT-Cloud device in the vineyard using Long Range (LoRa) wireless technology. The TT-Cloud then relays the data to a computer server through the internet via a General Packet Radio Service (GPRS) network. At the time of this study, the TTWs were operating on software version 2.1. The integration time of the TTWs was set to 50 minutes, and the gain was equal to 3. The TTWs took continuous, hourly measurements for the duration of their deployment.

Focusing on the light transmission measurement, the TTW system employs the same spectral sensor chips used in the TT system to monitor the visible to near-infrared electromagnetic spectrum that is transmitted through the canopy. Each TTW is equipped with two chips, each collecting six bands of data. The AMS AS7262 spectrometer chip covers the visible range (450–650 nm) with bands (40 nm bandwidth) centered at 450, 500, 550, 570, 600, 610, and 650 nm. The AMS AS7263 spectrometer chip covers the NIR range (610–860 nm) with bands (20 nm bandwidth) centered at 680, 730, 760, 810, and 860 nm (Tomelleri et al., 2022). These chips are mounted on the top of the TTW and have a 40° field of view (FOV).

## 2.2 Field deployment of TTWs

### 2.2.1 Site Description

This research was conducted in 2023 in three commercial vineyards in Niagara, Ontario, Canada, in the Niagara Escarpment appellation. The vineyards used for the in-field TTW deployment for monitoring vine health are both managed by the same winery. The first site where vine health was monitored, referred to as ON_VIN_01 in this study, is in the sub-appellation of the Beamsville Bench (43° 9'59.08"N, 79°29'50.62"W) with the second location, known as ON_VIN_012, 10.6 km away in the sub-appellation of Twenty Mile Bench (43° 7'45.99"N, 79°22'40.16"W). The third site, ON_VIN_03, was used to harvest fruit samples throughout the growing season to monitor grape TSS development with NIR analysis. ON_VIN_03 is located directly across the road from ON_VIN_01 in the sub-appellation of the Beamsville Bench (43° 9' 56.49" N, 79° 29' 49.47" W). Site locations are shown in Figure 2-1. Both ON_VIN_01 and ON_VIN_02 are outfitted with meteorological data. Weather data for ON_VIN_03 was obtained from the meteorological station at ON_VIN_01, due to sites proximity to each other (<500m).

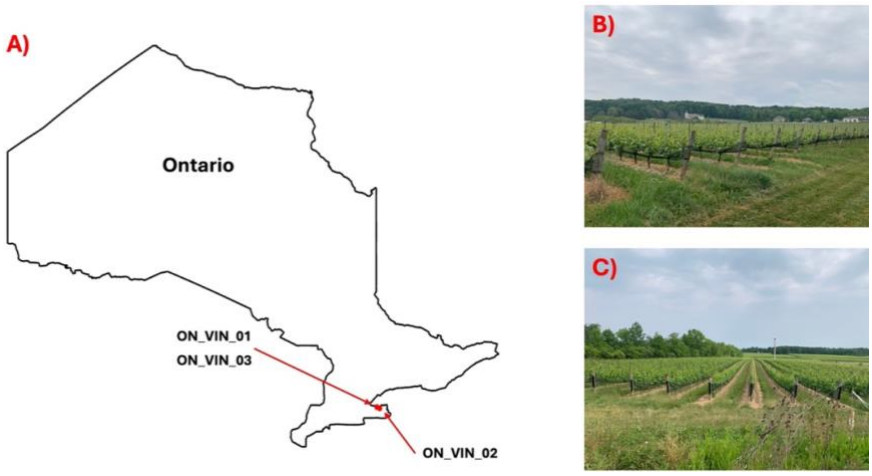


**Figure 2-1:** A) Location of ON_VIN_01 and ON_VIN_02 in the Niagara Escarpment appellation, in Niagara, Ontario, Canada. B) Photograph of ON_VIN_01 on June 9th, 2023 (DOY 160). C) Photograph of ON_VIN_02 on June 9th, 2023 (DOY 160).

All meteorological data besides the precipitation data for ON_VIN_02 was obtained from meteorological stations that were maintained at both ON_VIN_01 and ON_VIN_02. $T_A$ was measured above the canopy (HMP155; Vaisala: Helsinki, Finland) and soil temperature was measured at 5cm depth (TCAV-L; Campbell Scientific: Logan, UT, USA). Rainfall was measured half-hourly using a weighing bucket precipitation gauge (AEPG 600, Belfort Instrument Company, Baltimore, MD, USA) and was placed in a clear area to avoid interception from the vines. Meteorological data at both ON_VIN_01 and ON_VIN_02 was logged as a mean half-hour to a Sutron data logger (XLite 9210B, Sutron Corporation, Virginia, USA).

In 2023, the average air temperature ($T_A$) at ON_VIN_01 and ON_VIN_03 was 11.0 °C, with soil temperatures of 12.3°C, and 806 mm of precipitation received. The soil is described as Chinguacousy – Loamy Phase (OMAFRA GIS, 2019). Soil at ON_VIN_02 is described as Cashel (OMAFRA GIS, 2019). At ON_VIN_02, the 2023 average $T_A$ was 10.6°C, with soil temperature of 11.8°C, and 620.3 mm of precipitation (Environment and Climate Change Canada, 2023). For ON_VIN_02 precipitation data from a government-maintained weather station Vineland Station, Ontario (43°11'00.000" N, 79°24'00.000" W) was used as it was the closest full record in the same sub-appellation. The rain gauge at ON_VIN_02 malfunctioned during the growing season and therefore the precipitation data was incomplete. ON_VIN_01 precipitation data could not be used for ON_VIN_02 as the two sites are in two different sub-appellations.

The 30-year climate average for the region (1991–2020), as established by Environment and Climate Change Canada, indicates that the typical annual precipitation is 838 mm, with an average of 436 mm during the growing season, from May 1st (DOY 121) to October 31st (DOY 304) (Environment and Climate Change Canada, 2024). During the 2023 growing season, ON_VIN_01 recorded 423 mm of precipitation, slightly below the seasonal average. In contrast,

the Vineland Station meteorological tower, as a proxy for ON_VIN_02, received 373 mm of precipitation during the same growing season period, 63 mm less than the regional 30-year average for the growing season. $T_A$ during the 2023 growing season was also slightly elevated than that of the 30-year average of 9.4°C, with an increase of 1.6°C at ON_VIN_01 and 1.2°C at ON_VIN_02 (Environment and Climate Change Canada, 2024).

All vineyard sites are non-irrigated and managed in a double Guyot on a vertical trellis with a north–south orientation, with a vine spacing of 1 m and row spacing of 2.4 m. Each vineyard is comprised of multiple varieties of *V. vinifera CV* and organized into variety specific blocks. At ON_VIN_01 and ON_VIN_02 monitoring was focused on *V. vinifera CV* Cabernet Franc blocks, which were established in 2015 at both vineyard locations. Bird netting was used in both blocks during veraison to protect the berries from predation. At ON_VIN_03 *V. vinifera CV.* Cabernet Franc, Chardonnay and Riesling, established in 2000, 2000 and 2009 respectively, whole clusters were collected at regular intervals. All blocks were maintained with the use of standard practices of the region, however Cabernet Franc at ON_VIN_03 was cultivated organically.

### 2.2.2 Vine Health Monitoring

The TTW system was deployed in the Cabernet Franc blocks at ON_VIN_01 and ON_VIN_02 on May 17$^{th}$, 2023 (DOY 137), just after bud break on the vines. In each designated monitoring block within the vineyards, a row of vines was randomly selected for TTW installation. Four vines per row were chosen based on trunk suitability for sap flow sensor installation. Note that sap flow data is explored in a different study. As a result, eight TTWs were deployed for the study. The TTWs were secured to a mounting plate, which was attached to a bracket fixed to a T-bar near the vine (Figure 2-2). Each TTW was positioned below the canopy to ensure that the spectral sensors had a clear view of the foliage. When the T-bar was too far from the vine for

proper sensor positioning, the TTWs were mounted on the end of a threaded rod serving as an extender. To accommodate this, the mounting brackets were modified with welded nuts so the rod could be threaded into the bracket for support and full reach. The battery and solar panel packs were mounted above the canopy using a custom-fabricated unit on the same T-bar (Figure 2-2).


**Figure 2-2**: A) A TTW sensor deployed to monitor a Cabernet Franc vine at ON_VIN_01, supported by a rod attached to a T-bar used in the trellis system. The battery is positioned above the canopy to keep the solar panel free from vine cover. B) A close-up of the TTW sensor positioned under the canopy.

Since the TTW system was deployed in a commercial vineyard, several uncontrollable variables related to vine maintenance could affect the positioning and functioning of the TTW and resulted in some data gaps. Additionally, the original TT system reports sensor failures due to water intrusion and low battery charge (Vaglio Laurin et al., 2024). To minimize the risk of instrument failure, the TTWs were regularly inspected throughout the growing season. Inspections ensured that the positions had not shifted due to activities like hedging, pruning, or bird netting installation. The sensors' FOV was cleaned to prevent obstruction from dust, pollen and spray residues. TTW batteries were replaced if needed, and units were checked for signs of water

intrusion. The battery and solar panel packs were also routinely checked to make sure the solar panels were clear from dust and spray residue, along with trying to minimize vine interference with the solar panels.

## 2.3 Lab deployment of TTWs

To create consistent environmental conditions, an experiment was run inside a Plant Growth Chamber (BioChambers, Canada), where $T_A$, relative humidity and artificial sunlight were kept constant. To match typical growing conditions in vineyards surrounding grape clusters, $T_A$ was kept at 20 °C, and relative humidity was kept at 70%. Three racks were custom fabricated to be used in the plant growth chamber where the TTWs can be mounted to the base and the grape clusters suspended directly above the sensors at varying distances (Figure 2-3).

**Figure 2-3:** A photograph of the rack system that was used to support the grape clusters over top of the TTWs in the Plant Grow Chamber for monitoring grape maturity.

### 2.3.1 Optimizing Fruit to Sensor Distance

This portion of the experiment was done prior to the 2023 growing season. As such, grapes from local, commercial wine vineyards were not available to use. As a substitute, table grapes, both green and red skinned, were purchased from grocery stores and used to calibrate the optimal

distance. Grapes were suspended 0, 4, 6, 10 and 15 cm from the TTW top, with the last TTW on the rack being left open as a control, as visualized in Figure 2-4. Three of the custom fabricated racks were placed in the plant growth chamber to run the experiment in triplet. Afterwards, the collected spectral data from the sensors were analyzed to determine the distance at which oversaturation occurred.

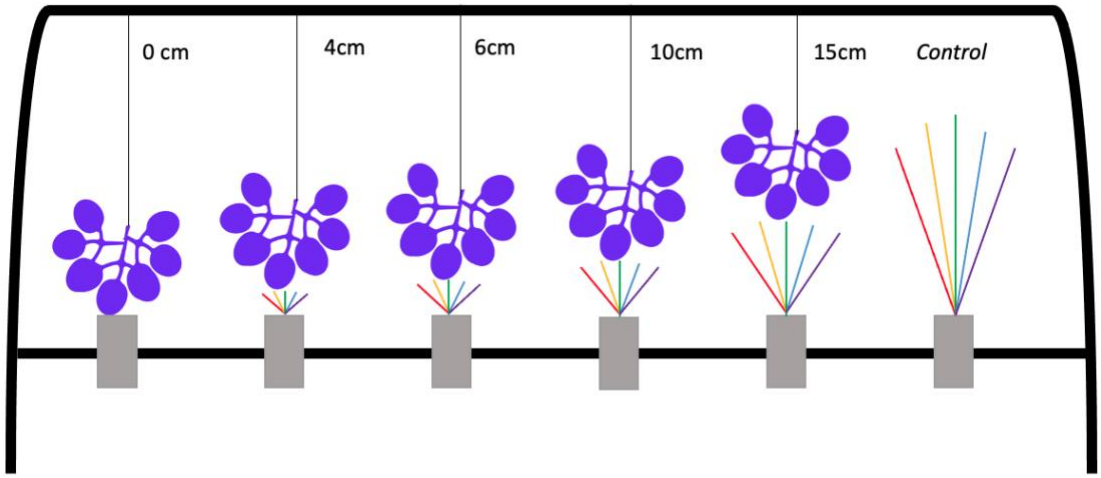


**Figure 2-4:** Experiment configuration for determining the optimal distance between the fruit clusters and the sensor lenses.

### 2.3.2 Grape Maturity Monitoring

Grape samples were collected bi-weekly from ON_VIN_03 starting at the pea size stage on August 1, 2023 (Day of Year [DOY] 213), continuing until veraison on September 8, 2023 (DOY 251). Following veraison, grapes were collected weekly until harvest of each specific variety. As seen in Figure 2-5(A). After sample collection in the field, the grape clusters were immediately transported to the laboratory for spectral signature collection. The grape clusters were not washed prior to data collection in order to preserve any potential residues that may occur in field conditions. Each grape cluster was weighed and suspended over the sensors, ensuring that the cluster was in direct contact with the sensor, as shown in Figure 2-5(B). Hourly spectral readings

were taken using the TTWs in a plant growth chamber, programmed according to predetermined parameters to simulate daytime growing conditions. The sensors were left to operate overnight for approximately, 12 hours.

Subsequently, each grape cluster was individually de-stemmed, juiced using a centrifugal juicer (Breville, Canada), and filtered through cheesecloth and coffee filters to obtain a clear juice sample free of solids, as seen in Figure 2-5(C). The filtered juice samples were then refrigerated overnight. The following day, TSS was measured in °Brix, of the must samples were determined using a Lyza 5000 refractometer (Anton Paar, Canada).

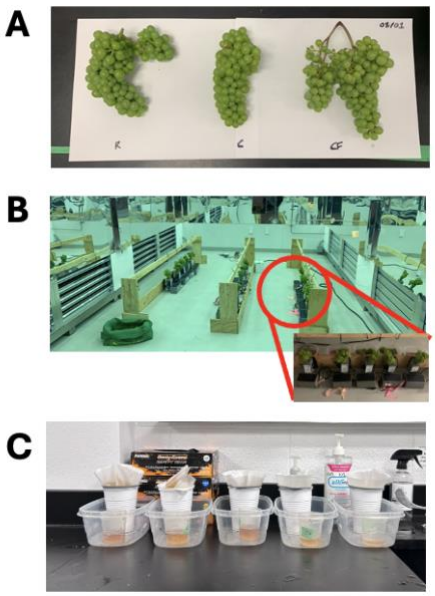


**Figure 2-5:** A) Grape clusters were collected biweekly from the time berries formed on the vines and continued through to harvest. Collection frequency increased to weekly after the onset of veraison. B) Grapes clusters were transported back to the laboratory and suspended overtop of the sensors in a Growth Chamber for 12 hours, measured every hour. C) The following day, the grape clusters were individually juiced and filtered. Samples were refrigerated overnight and then °Brix readings were taken at a partner vineyard using the Lyza 5000 Wine.

## 2.4 Data Analyses

As the TT Cloud was not used in this study, the data was manually downloaded from each TTW using the external connection on the device. As outlined in both the TTW system manual and Vaglio Laurin et al. (2024), digital numbers (DN) that were greater than 65000 were exclude from

the dataset, as that indicates that the values are oversaturated and not accurate. The TTWs store the spectral readings as radiometrically uncalibrated data, and therefore, the spectral bands are not directly comparable to each other and must be converted into energy values for accurate comparison. The DNs for each band $(i)$ were then converted into energy (E) values of $\frac{10^{-6}W}{cm^2}$, using Equation 2 and calibration factors (CF) from Belelli Marchesini et al. (2023) which are presented in Table 2-1. Note that Equation 2 is valid only when TTW system is set to a gain of 3.

$$E_i = \frac{DN_i}{4 * CF_i} \quad (2)$$

**Table 2-1:** Calibration factors (CF) for each band length $(i)$ of the TTWs, which are used to convert Digital Numbers (DN) into energy values (E) as described in Equation 2.

| **Wavelength (nm) $(i)$** | **Calibration Factor (CF)** |
|---|---|
| 450 | 2214.6 |
| 500 | 2002.7 |
| 550 | 1715.4 |
| 570 | 1690.9 |
| 600 | 1605.8 |
| 610 | 919.1 |
| 650 | 1542 |
| 680 | 957.1 |
| 730 | 943.2 |
| 760 | 915.2 |
| 810 | 1000.9 |
| 860 | 994.3 |

### 2.4.1 NDVI Calculations with TTW Spectral Data

As noted in Stamford et al. (2023), while NDVI is widely used, there is no universally agreed-upon standard for the specific red and NIR wavelengths used in its calculation. In the present study, a red band at 650 nm and a NIR band at 860 nm from the TTW system were selected for $NDVI_T$.

These bands were chosen as they are closest to the bands used by S2 for NDVI calculation: 665 nm (red) and 842 nm (NIR) (Pour et al., 2023).

Therefore, using the 650 nm and 860 nm bands of the TTW, $NDVI_T$ was calculated using:

$$NDVI_T = (860nm - 650nm)/(860nm + 650nm) \quad (3)$$

The daily maximum $NDVI_T$ value of each TTW was selected for each day, and then the sensors in each monitoring block were averaged together to determine daily and weekly $NDVI_T$ values for each block.

### 2.4.2 Satellite Imagery

The Sentinel-2 (S2) satellites that are a part of the Copernicus program were used to gather additional NDVI measurements of the study location, measuring light that is reflected from the canopy. The S2's 10-20 m spatial resolution along with 13 spectral bands ranging from 443-2190 nm, is a commonly used satellite to monitor vine vigor and health throughout the growing season (Mucalo et al., 2024; Pour et al., 2023). Atmospherically corrected S2 images that were cloud (<30% cloud cover) and smoke free products for our study row at both ON_VIN_01 and ON_VIN_02 over the study period were obtained through Google Earth Engine (Gorelick et al., 2017). NDVI of each image was then subsequently computed, using harmonized bands 4 (655 nm) and 8 (842 nm) of S2:

$$NDVI = (Band\ 8 - Band\ 4)/(Band\ 8 + Band\ 4) \quad (1)$$

### 2.4.3 Development of TSS Prediction Models

For each grape variety, a Partial Least Squares (PLS) regression model was developed to yield three unique models. PLS models operate by determining what combination of independent

variables best predicts the dependent variable using regression (Zifarelli et al., 2020). PLS is a widely accepted method for linking spectral signatures, independent variable, with grape TSS, as measured by °Brix, the dependent variable (Benelli et al., 2021; Ebrahimi et al., 2024; Fernández-Novales et al., 2019a; Santos-Campos et al., 2023). The relationship between spectral bands and TSS, over the maturation period of the 2023 growing season was established using the laboratory-based TTW measurements and corresponding TSS readings.

Most PLS models for grape maturity predictions only utilize the NIR light range with wavelengths from 780 to 2500 nm (Ferrara et al., 2022b; Urraca et al., 2016; Walsh et al., 2020). However, Swe et al. (2023) found that light within the 700–800 nm range was particularly effective for predicting TSS in grapes. Similarly, Gomes et al. (2017) identified the 740–770 nm range and 840 nm as being especially useful for TSS prediction. Further, Giovenzana et al. (2014) emphasized the importance of wavelengths around 670 nm, as well as 730 and 780 nm, for assessing grape maturity using NIR spectroscopy.

Although 610 nm, 680 nm and 730 nm fall outside the traditional NIR spectrum this study incorporated these wavelengths into the models to explore their potential associations with TSS development in grapes. This decision was based on evidence supporting their relevance and the capability of the TTW spectrometers to capture readings in these wavelengths (Giovenzana et al., 2014; Gomes et al., 2017; Swe et al., 2023). While many studies include spectral wavelengths in the 900-1000 nm range to monitor fruit maturity (Benelli et al., 2021; Ebrahimi et al., 2024; Walsh et al., 2020), bands above 860 nm were excluded from the model due to limitations of the TTW sensor. In addition to spectral data, $T_A$ was included in the models, recognizing its strong correlation with grape maturity (Jackson and Lombard, 1993). Although precipitation is known to directly affect grape composition, including TSS concentration (Esteban et al., 2002), precipitation

was not included as a variable in the PLS models, as the grape collection dates did not align with rain events, therefore, there was not enough data to incorporate into the models.

As such, the final PLS models used in this study incorporated spectral values collected by TTWs at 610, 680, 730, 760, 810 and 860 nm along with °Brix measurements for each grape cluster, and with daily average $T_A$ for the day of collection. A Variable Importance in Projection (VIP) threshold of 0.8 was employed to identify variables with significant influence on model prediction, ensuring that only the most impactful variables were retained in the final models (Fernández-Novales et al., 2019a).

### 2.4.4 Data processing software

All of the TTW data processing was performed using R Studio (R Core Team, 2021). The R packages used include: *dplyr* (Wickham et al., 2023), *ggplot2* (Wickham, 2016) and *pls* (Liland et al., 2023).

# Chapter 3: Results

## 3.1 Field-Based Monitoring of Vine Health Using TTWs

### 3.1.1 Overview of $NDVI_T$ Trends Across Vineyards

TTW were deployed for a total of 191 days in the vineyard, collecting data hourly. As a result, 4550 data points were collected per vine. Due to the large amount of data, daily maximum $NDVI_T$ was calculated for each TTW, before daily and weekly average $NDVI_T$ was calculated for each vineyard. Figure 3-1 illustrates the daily maximum $NDVI_T$ values for each of the deployed TTWs throughout the growing season. TTW 2 at ON_VIN_01, malfunctioned and has subsequently been removed from further data analysis. Additionally, TTW 4 at ON_VIN_02 has also been removed from further data analysis due to the value drift that occurred after hedging. The monthly average $NDVI_T$ values are summarized in Table 3-1 for both sites.

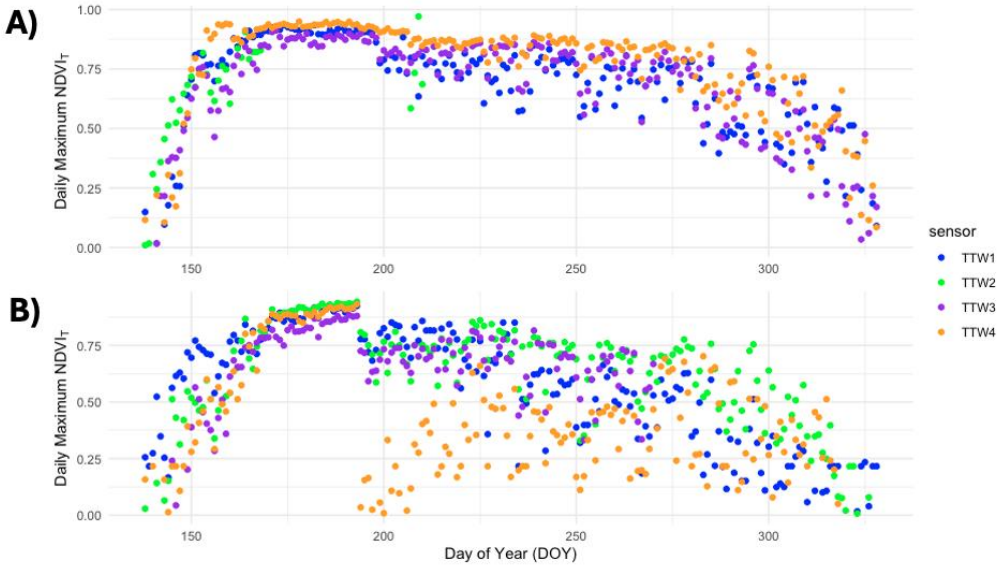


**Figure 3-1: A)** Daily maximum $NDVI_T$ for the 2023 growing season (May 9, 2023 – November 24, 2023) at TTW locations deployed at ON_VIN_01. TTW 1, TTW 2, TTW 3, and TTW 4 are represented by blue, green, purple, and orange dots, respectively. Decrease observed on DOY 199 aligns with vineyard maintenance. **B)** Daily maximum $NDVI_T$ for the 2023 growing season (May 9, 2023 – November 24, 2023) at TTW locations deployed at ON_VIN_02. TTW 1, TTW 2, TTW 3, and TTW 4 are represented by blue, green, purple, and orange dots, respectively. Decrease observed on DOY 194 aligns with vineyard maintenance.

**Table 3-1:** Average monthly $NDVI_T$ values for the 2023 growing season at ON_VIN_01 and ON_VIN_02.

| Month | May | June | July | August | September | October |
|---|---|---|---|---|---|---|
| Day of Year | 130 -152 | 153-182 | 183-213 | 214-244 | 245-274 | 275-305 |
| ON_VIN_01 | 0.28 | 0.85 | 0.86 | 0.76 | 0.76 | 0.62 |
| ON_VIN_02 | 0.25 | 0.74 | 0.79 | 0.69 | 0.58 | 0.44 |

To provide a more comprehensive overview of the vineyards, daily $NDVI_T$ values were averaged for each site (Figure 3-2). Initially, $NDVI_T$ was observed to be 0 at both vineyard sites when the TTWs were first deployed. Over the course of the growing season, the maximum $NDVI_T$ for ON_VIN_01 reached 0.92 on DOY 172, while ON_VIN_02 reached a maximum $NDVI_T$ of 0.91 on DOY 193. Despite ON_VIN_01 achieving its maximum $NDVI_T$ on DOY 172, daily $NDVI_T$ remained between 0.89 and 0.91 until DOY 199. At this point, the vineyard was hedged, causing $NDVI_T$ to decrease drastically overnight, though it remained stable afterward. On DOY 258, daily maximum $NDVI_T$ began to decrease rapidly as the vines entered senescence. A similar pattern was observed at ON_VIN_02; however, two main differences were noted. First, the highest daily maximum $NDVI_T$ was recorded the day before the vineyard was hedged and leaves were removed from around the fruiting zone. Secondly, the overall daily maximum $NDVI_T$ values are lower than that observed at ON_VIN_01. In general, at both sites, the standard deviation for the daily maximum $NDVI_T$ was low, except during senescence, when greater variation in $NDVI_T$ was observed between the TTWs.

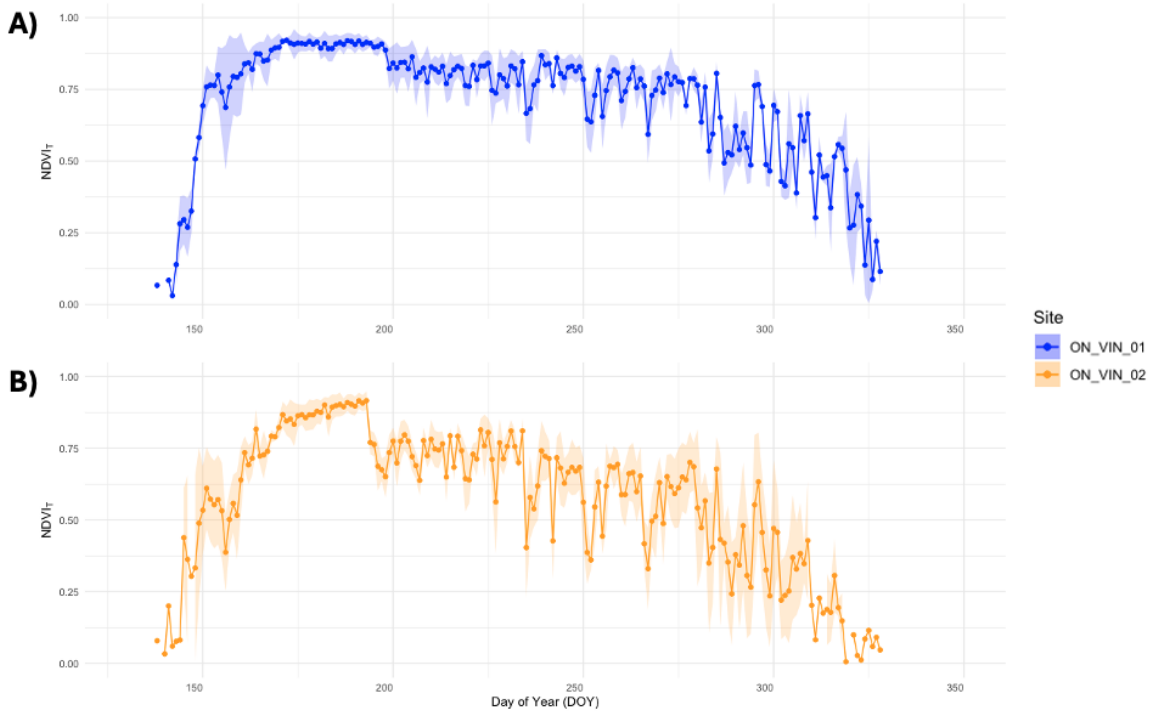


**Figure 3-2:** A) Average daily maximum $NDVI_T$ for the 2023 growing season (May 9, 2023 – November 24, 2023) at ON_VIN_01. The averages for ON_VIN_01 were calculated using TTW 1, TTW 3, and TTW 4. Standard deviation is illustrated as the shaded region. Decrease observed on DOY 199 aligns with vineyard maintenance. B) Average daily maximum $NDVI_T$ for the 2023 growing season (May 9, 2023 – November 24, 2023) at ON_VIN_02. The averages for ON_VIN_02 were calculated using TTW 1, TTW 2, and TTW 3. Standard deviation is illustrated as the shaded region. Decrease observed on DOY 194 aligns with vineyard maintenance.

### 3.1.2 Patterns of $NDVI_T$, Temperature, and Precipitation

Overall, the large volume of continuous data revealed noticeable trends when examining the maximum $NDVI_T$ on a weekly scale throughout the growing season (Figure 3-3). In general, the $NDVI_T$ followed a similar trend to the weekly average air $T_A$ at both sites. At the beginning of the growing season, $NDVI_T$ increased along with average $T_A$. $NDVI_T$ remained stable during the middle of the growing season, which coincided with sustained high $T_A$ between weeks 27 and 35. Once $T_A$ started to decrease, $NDVI_T$ also began to decline. In the latter half of the growing season, more variation in $NDVI_T$ was observed. However, these increases in $NDVI_T$ generally aligned

with periods of rising $T_A$ or when significant precipitation was recorded, particularly in weeks 40 and 43.


**Figure 3-3:** A) Weekly maximum $NDVI_T$ for the 2023 growing season at ON_VIN_01 (blue) and ON_VIN_02 (orange), spanning May 13, 2023 to November 24, 2023. The dashed line indicates when hedging and leave remove in the fruiting zone occurred at each study site, the colour corresponded to the location. B) Weather data for the 2023 growing season at both study sites, spanning May 13, 2023 to November 24, 2023. Average weekly Air Temperature (°C) is represented by the line on the primary y-axis, and weekly precipitation (mm) is shown as bars on the secondary y-axis. Colour represents the site, with ON_VIN_01 in blue and ON_VIN_02 in orange. Air temperature and precipitation data for ON_VIN_01, along with air temperature at ON_VIN_02 are from meteorological stations maintained on site. Precipitation data for ON_VIN_02 is from a nearby, government maintained station in Vineland Station (Environment and Climate Change Canada, 2023).

### 3.1.3 Comparison of TTW $NDVI_T$ and S2 NDVI Measurements

During the growing season, six days of S2 data were collected at ON_VIN_01, and five days of S2 data were collected at ON_VIN_02. The NDVI values calculated with the S2 data are summarized in Table 3-2. Overall, daily maximum $NDVI_T$ values tended to be higher than those calculated using S2 data at ON_VIN_01, with an absolute average discrepancy of 0.23 between the two methods. At ON_VIN_02, the difference between the methods was less pronounced, with an absolute average discrepancy of 0.15, although daily maximum $NDVI_T$ values still trended

higher than S2 NDVI values. The absolute average difference in NDVI measured by TTW and S2 is shown in Figure 3-4 for each day of S2 data.

**Table 3-2:** NDVI values calculated from the Sentinel-2 satellite for each day during the 2023 growing season at ON_VIN_01 and ON_VIN_02, excluding days with cloud cover or wildfire smoke. Shading indicates days when cloud cover prevented accurate measurements at the other site.

| Day of Year | **141** | **146** | **151** | **156** | **176** | **216** | **226** | **246** |
|---|---|---|---|---|---|---|---|---|
| **ON_VIN_01** | 0.4744 | 0.4706 | | 0.439 | 0.5787 | | 0.5875 | 0.7919 |
| **ON_VIN_02** | | 0.44258 | 0.4696 | | 0.5911 | 0.7758 | 0.5576 | |

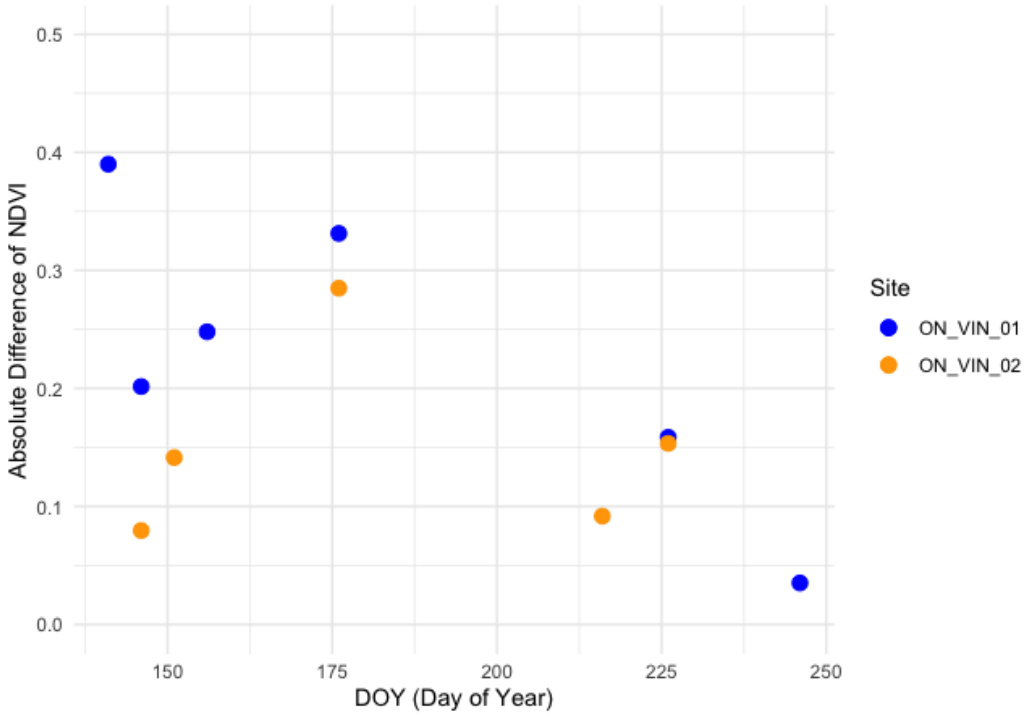


**Figure 3-4:** The absolute difference between $NDVI_T$ (calculated via TTW) and NDVI (calculated via S2) during the 2023 growing season at ON_VIN_01 (blue) and ON_VIN_02 (orange), spanning from May 21 to September 3, 2023.

## *3.2* Determining Spectral Relationships for Monitoring Grapes Maturity in the Lab

### 3.2.1 Optimal distance TTW Distance

The calibration of sensor-to-grape distance revealed that when grape clusters were positioned 4 cm or more from the sensor, the spectral readings became over-saturated, making the data unusable. In contrast, measurements taken with a sensor distance of 0 cm yielded valid data

without oversaturated values at any wavelength, indicating that for consistent measurements grape clusters need to be placed directly over top of the TTWs. Table 3-3 summarizes digital numbers for each distance tested. Based on these findings, subsequent experiments in monitoring grape maturity were conducted with the grapes placed as close as possible to sensor, with the goal of achieving direct contact between the clusters and the sensor to ensure high-quality, consistent data.

**Table 3-3***:* Spectral readings from the distance experiment for each wavelength. Sensor distance refers to the distance between the grape cluster and the TTW, with the control not including a grape cluster. Over-saturated (OS) readings, shaded in the table, represent values greater than 65000.

| **Wavelength (nm)** | **Sensor Distance (cm)** | | | | | |
|---|---|---|---|---|---|---|
| | **0** | **4** | **6** | **10** | **15** | **Control** |
| 450 | 1253 | 16376 | 8448 | 8714 | 18895 | 46268 |
| 500 | 1817 | ***OS*** | 9780 | 40403 | ***OS*** | ***OS*** |
| 550 | 4442 | ***OS*** | ***OS*** | ***OS*** | ***OS*** | ***OS*** |
| 570 | 5588 | ***OS*** | ***OS*** | ***OS*** | ***OS*** | ***OS*** |
| 600 | 8636 | ***OS*** | ***OS*** | ***OS*** | ***OS*** | ***OS*** |
| 610 | 2500 | ***OS*** | 20716 | 20096 | 27693 | ***OS*** |
| 650 | 2207 | ***OS*** | 10280 | 15344 | 38886 | ***OS*** |
| 680 | 795 | 14906 | 4330 | 9834 | 13590 | 18246 |
| 730 | 1196 | 4778 | 2633 | 4909 | 5650 | 9496 |
| 760 | 1950 | 10109 | 3354 | 7227 | 10838 | 8524 |
| 810 | 6887 | ***OS*** | 11089 | 20238 | 23592 | 26915 |
| 860 | 1362 | 5823 | 2968 | 3727 | 5917 | 6283 |

### 3.2.2 TSS Development in Sample Grapes

During the 2023 growing season, a total of 130 grape clusters were harvested across three grape varieties. Chardonnay reached full maturity the earliest, with an average °Brix of 19.72 on DOY 277 (October 4, 2023), the day prior to harvest, following seven sampling campaigns. In contrast, Cabernet Franc matured the latest, with an average °Brix of 20.91 on the day before harvest on DOY 305 (November 1, 2023), after 11 sampling campaigns. Riesling, harvested on DOY 288 (October 15, 2023), after eight sampling campaigns, had an average °Brix of 17.50 on the day

before harvest. A comprehensive statistical summary of the TSS values for each grape variety is provided in Table 3-4.

**Table 3-4*:*** Statistical information for the Total Soluble Solids (TSS) data collected per cluster, measured as °Brix, throughout the 2023 growing season for the monitored varieties at ON_VIN_03.

| | **Minimum** | **Maximum** | **Median** | **Mean** | **Standard Deviation** | **Number sampling campaigns** |
|---|---|---|---|---|---|---|
| **Cabernet Franc** | 3.49 | 22.31 | 17.71 | 15.50 | 6.23 | 11 |
| **Chardonnay** | 3.49 | 22.55 | 16.04 | 14.09 | 5.97 | 7 |
| **Riesling** | 3.31 | 19.31 | 14.77 | 12.98 | 5.51 | 8 |

### 3.2.3 Model Performance and Accuracy

To evaluate how much each predictor contributes to explaining TSS for each PLS model, a VIP factor threshold of 0.8 was used. Variables that had a VIP score higher than 0.8 were determined to be the important for the PLS to use for the TSS predication of each grape variety. For Cabernet Franc, the wavelengths 680 and 730 nm, and $T_A$ were key predictors for TSS. In Chardonnay, the significant predictors included wavelengths of 680, 760 and 860 nm, along with $T_A$. For Riesling, the most important wavelengths were 610, 680, 760, 810, and 860 nm. Results are summarized in Table 3-5.

**Table 3-5:** Variables assessed for importance in the Partial Least Squares (PLS) model. Variables that were included in the final model for each variety are indicated with a checkmark.

| Model Variable | | Cabernet Franc | Chardonnay | Riesling |
|---|---|---|---|---|
| **Wavelength** | **Light Region** | | | |
| 610 nm | Visible | $x$ | $x$ | ✓ |
| 680 nm | Visible | ✓ | ✓ | ✓ |
| 730 nm | NIR | ✓ | $x$ | $x$ |
| 760 nm | NIR | $x$ | ✓ | ✓ |
| 810 nm | NIR | $x$ | $x$ | ✓ |
| 860 nm | NIR | $x$ | ✓ | ✓ |
| Air Temperature ($T_A$) | | ✓ | ✓ | $x$ |

Among the PLS models developed to predict TSS throughout the growing season, the Cabernet Franc model demonstrated the highest accuracy, explaining 59% of the variance ($R^2 = 0.59$) and yielding an average error of 4.12 °Brix (RMSEP = 4.12). The Riesling model followed, with an $R^2$ value of 0.52, while the Chardonnay model exhibited the lowest accuracy, with an $R^2$ value of 0.41. These results are visually represented in Figure 3-5. Indicators of a robust predictive model include an $R^2$ value as close to 1.0 as possible and low RMSEP values (Benelli et al., 2021; Ferrara et al., 2022a). While the RMSEP values for the models are relatively low, the $R^2$ values are somewhat further from 1.0 than would typically be expected for highly accurate models, particularly for the Chardonnay model.

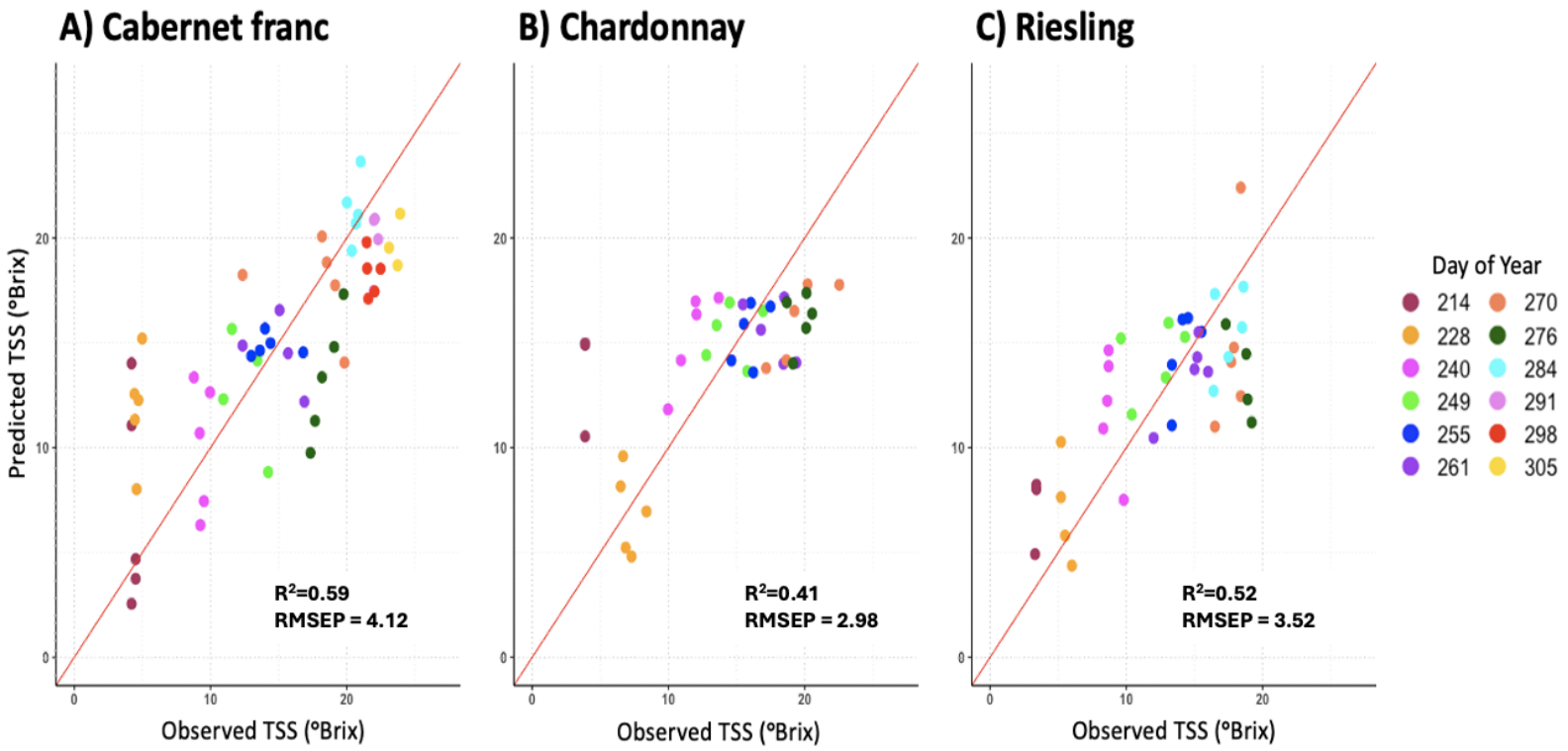


**Figure 3-5:** Visual representation of the accuracy of PLS models for three grape varieties: Cabernet Franc (A), Chardonnay (B), and Riesling (C). Variables included in each model differ depending on the variety, as described in Table X. Observed Total Soluble Solids (TSS; as measured in °Brix) values are plotted on the x-axis, and PLS-predicted Total Soluble Solids (TSS; as measured in °Brix) values are plotted on the y-axis. The red line represents the 1:1 ratio. Dot colours correspond to the day of the year when the grape samples were collected.

# Chapter 4: Discussion

## 4.1 Using TTWs to monitor vine health

### 4.1.1 $NDVI_T$ Variability and Influencing Factors

While there was generally agreement among the TTWs across the vineyards, the standard deviation increased at the end of the growing season. This discrepancy can likely be attributed to senescence and variations in the rate at which individual leaves progress through the process. Leaf senescence, the final stage of leaf development, is a highly coordinated process where leaves change colour, reflecting chlorophyll loss, and ends with the death of the leaf (Guo et al., 2021; Li et al., 2023). However, there is limited literature addressing the rates of senescence in vineyards, primarily due to two factors: (i) the processes driving leaf senescence remain poorly understood. While stress-response pathways and environmental triggers have been identified, the overall understanding is still incomplete (Delpierre et al., 2009; Guo et al., 2021); and (ii) the large-scale measurement practices commonly used in NDVI assessments limit the ability to capture vine differences and fine-tune spatial variability in senescence.

The primary and most influential environmental factor that has been identified to be in relation to leaf senescence is shading and darkness (Li et al., 2023). Thimann (1985) reports that leaves placed in dark or brightly lit environments do not senesce at the same rate. Specifically, leaves in dark conditions undergo senescence more quickly, while those exposed to high light levels experience a delay in this process. Additionally, it was observed that when only part of a leaf is covered, the shaded portion progresses through senescence at the rate associated with darkness, while the uncovered portion senesces more slowly, at the rate associated with light (Thimann, 1985). Given the dense canopy structure of vineyards, it is reasonable to assume that

vine leaves are subject to varying degrees of shading and, consequently, will progress through senescence at different rates.

Gatti et al. (2017) support this argument as they find that leaves in high-density canopies tended to enter senescence earlier than those in other areas of the same vineyard. Additionally, as observed in the field during senescence in this study, chlorophyll degradation within the canopy was not uniform as indicated with the green to yellow colour change, with more advanced chlorophyll loss being concentrated in the middle of the canopy where there would be a high level of shading (Figure 4-1). Consequently, $NDVI_T$ values during this period would reflect varying states of chlorophyll degradation, depending on the section of the canopy within the FOV of the TTWs. This variability likely contributed to the increased standard deviations observed during this period.

**Figure 4-1:** A photograph of the canopy from a site visit to ON_VIN_01 on October 26, 2023 (DOY 299). Some leaves had entered senescence, resulting in yellowing foliage, while other leaves remained green, indicating that chlorophyll degradation had not yet begun in those leaves.

Other variation among the TTWs was noted in TTW 4 at ON_VIN_02, after DOY 194. This is likely due to hedging, a vineyard management practice that removes leaves to focus vine energy on fruit production (Freeman and Cullis, 1981), along with the leaf removal from around the fruiting zone, a vineyard management practice that decreases disease pressure by increasing air flow around the fruit (Smart, 1985). Therefore, it is hypothesized that the removal of leaves during these vineyard management practice caused ON_VIN_02 TTW 4 to be positioned too far from the canopy to capture accurate readings. Although no photographs of TTW 4 at ON_VIN_02 are available, the magnitude of the canopy change is evident in Figure 4-2. Note that major readjustments to the sensors position to compensate for vineyard maintenance are limited as the TTWs were attached to the vine to monitor sap flow as part of a different study.


**Figure 4-2:** A) A TTW sensor positioned under the Cabernet Franc canopy at ON_VIN_01 to monitor vine health. Photographed DOY 180 (June 29th, 2023), approximately two weeks before hedging and leaf removal from the fruiting zone. B) the same Cabernet Franc vine a week later after canopy maintenance, leaving a large distance between the canopy and the sensor. Photographed DOY 207 (July 26, 2023).

## 4.2 $NDVI_T$ and Traditional NDVI Patterns

The $NDVI_T$ values calculated from TTWs follow a pattern consistent with traditional NDVI values derived from reflected light. As described by Wardlow et al. (2007), summer crops typically undergo a green-up period in the spring, characterized by rapid canopy development and a corresponding increase in NDVI. After the green-up phase, the progression of NDVI slows before reaching a peak and stabilizing. During senescence, NDVI values decrease abruptly due to chlorophyll loss and leaf drop (Wardlow et al., 2007).

At both sites, the average $NDVI_T$ values closely follow this general pattern, with some expected deviations. Specifically, peak $NDVI_T$ occurs earlier, followed by a sharp decrease, before transitioning to a longer stable period. The decrease in $NDVI_T$ was observed on DOY 199 at ON_VIN_01 and DOY 194 at ON_VIN_02. This decrease aligns with the vineyard maintenance event of hedging, during which a significant portion of the canopy is removed to redirect the plant's energy toward fruit production rather than vegetative growth (Freeman and Cullis, 1981). As such, the deviations observed are consistent with the management practices occurring in the vineyards which differ from most summer crops and thereby causing the deviation from the traditional NDVI progression. Additionally, the observation of a quick $NDVI_T$ decrease after hedging at both ON_VIN_01 and ON_VIN_02 suggest that $NDVI_T$ is highly responsive to changes in the vine canopy. However, further investigation is needed to determine the full range of vine health conditions that TTWs can detect using $NDVI_T$.

### 4.2.1 Weather Effects on $NDVI_T$ and Vine Health

The 2023 growing season did not experience prolonged periods without precipitation or significant, unexpected disease pressure. As a result, the study was unable to demonstrate the ability of $NDVI_T$ to detect stressed vines under these conditions. However, a sharp increase in $NDVI_T$ was observed during weeks 40 and 43, coinciding with periods of increased $T_A$ and precipitation. These factors are known to affect plant productivity (Lieth, 1973), leading to an increase in chlorophyll within the vines. Since $NDVI_T$ is a ratio that measures the interaction of red light with chlorophyll in leaf cells, it is believed that the observed $NDVI_T$ increase reflects heightened plant productivity in response to these weather events. This is also supported by Yang et al. (1997) and Wang et al. (2003) who have found that NDVI values are highly correlated with precipitation and temperature, especially in the late growing season.

### 4.2.2 $NDVI_T$ Values and Comparison with Established NDVI Ranges

While there is no single standard classification system for NDVI values, values greater than 0.7 are generally associated with denser and healthier canopies due to increased chlorophyll content (Rous et al., 1973). As expected, the $NDVI_T$ values observed in this study fell into the mid 0.8 range in July and September at ON_VIN_01 and the mid to high 0.7 range at ON_VIN_02, which is a reasonable range for NDVI and indicates healthy vines. Wardlow et al. (2007) reported peak NDVI values of 0.73 for corn, 0.77 for sorghum, and 0.84 for soybeans, which fall within a similar range to those measured by the TTWs.

Looking at vineyards, Pãdua et al. (2019) reported NDVI values of 0.70, 0.82, 0.62, and 0.59 for DOY 137, 157, 190, 218, and 264, respectively, in a vineyard in Portugal. Similarly, Sun

et al. (2017) measured NDVI values in a California vineyard ranging from 0.50–0.70 on DOY 193, 0.60–0.70 on DOY 173, and 0.50–0.60 on DOY 253. The ranges of NDVI in Sun et al. (2017) represent the spatial distribution of values throughout the vineyards. The $NDVI_T$ values collected in this study, using the TTW sensor to measure light transmitted through the canopy, fall within a similar range to NDVI values calculated at both vineyard with reflected light, aligning with both general agricultural ranges and vineyard-specific values. This consistency suggests that $NDVI_T$ values provide an accurate representation of vine health using $NDVI_T$.

While the values of $NDVI_T$ fall within a similar range of NDVI, there was a discrepancy between $NDVI_T$, calculated by TTW, and NDVI, calculated by S2. $NDVI_T$ generally showed higher values than NDVI. NDVI, as calculated by S2, does not focus exclusively on the vines in the vineyard; instead, it also considers exposed soil and the inter-row cover, thus creating mixed pixels and influencing NDVI values with external factors. In contrast, $NDVI_T$ is positioned beneath the vine, so its sensor FOV captures only the canopy vegetation. A similar mismatch between S2 NDVI and TTW $NDVI_T$ was observed by Vaglio Laurin et al. (2024), who also noted that S2-derived NDVI did not align with $NDVI_T$, due to NDVI being influenced by mixed pixels. As a result, implementing $NDVI_T$, which can focus solely on the canopy of interest, has the potential yield highly accurate health metrics of vines, without interference from the inter-row cover crops.

Another advantage of TTW $NDVI_T$ compared to S2 NDVI is the data availability of $NDVI_T$. Although S2 has a high revisit rate due to the study sites high latitude (Jia et al., 2024; Mucalo et al., 2024), NDVI information from S2 was limited to six days at ON_VIN_01 and five days at ON_VIN_02 in the 2023 growing season as weather conditions significantly impacted the

ability of S2 to collect usable data. If clouds are present during the satellite's pass, the cloud cover can obstruct the view, preventing accurate NDVI calculations for the vegetation (Tarrio et al., 2020). Additionally, as seen in 2023 in the study region, wildfire smoke heavily impacted atmospheric conditions, further reducing the collection of reliable S2 data. In contrast, with $NDVI_T$, light does not need to be reflected back to a sensor. This means that atmospheric conditions, such as cloud cover or smoke, have less of an influence on the data, allowing for a more consistent and continuous dataset of vine health.

## 4.3 Monitoring Grape Maturity

### 4.3.1 Selection and Role of Spectral Bands in TSS Prediction Models

Overall, three models were developed to assess whether the TTWs could monitor and predict grape maturity through spectral analysis. Interestingly, each grape variety utilized a distinct set of spectral bands, with the 680 nm band being the only one used across all models. Given the association of the 680 nm band with chlorophyll absorption (Aronoff, 1950; Giovenzana et al., 2014; Walsh et al., 2020), the importance of this wavelength aligns with the physiological process of grape maturation. During the early stages of berry development, all grape varieties contain significant amounts of chlorophyll, which gradually transitions as the berries accumulate sugars, water, and organic acids (Giovanelli and Brenna, 2007; Robinson and Davies, 2000). Therefore, the models likely detected the decrease in chlorophyll content as the grapes matured.

In contrast to the models presented here, Benelli et al. (2021) did not find it necessary to include bands below 700 nm. However, their model was developed for monitoring berries later in the maturation process, when °Brix values were above 15, and thus, the influence of chlorophyll

content would have been much less significant. Similar to the models in the present study, Giovenzana et al. (2015) developed a TSS prediction model for Chardonnay grapes (a white variety) throughout the development process, with °Brix values as low as 5. They also found it important to include bands related to chlorophyll for TSS prediction, incorporating 630 nm and 690 nm in their model (Giovenzana et al., 2015). Swe et al. (2023) also found that in using hyperspectral imagining Rando grapes (a red variety) band 695 nm was used for TSS prediction. Interestingly, while the present study included two chlorophyll-related bands (610 and 680 nm), the Riesling model was the only one that found it necessary to include both.

All models in this study utilized bands in the 700-800 nm range. Golic et al. (2003) describe how, with increasing sucrose concentration, the 740 nm band decreases in intensity, while the 770 nm band increases, which is related to the OH vibrations in sugar and water content. In the current study, bands at 730 and 760 nm were used, as the 740 and 770 nm bands are not available on the TTWs. However, since TTWs have a sensitivity of ± 20 nm in the NIR range (Belelli Marchesini et al. 2023), the TTWs would still be able to detect changes in this wavelength range using bands 740 and 770 nm. None of the models in this study included both the 730 and 760 nm bands together for TSS prediction. However, the inclusion of these bands suggests that the models were capturing berry changes related to sugar development, reflecting the physiological processes involved in grape maturation.

Of particular interest, in their study of NIR spectroscopy, Giovenzana et al. (2015) used Chardonnay as the grape variety and selected bands at 630, 690, 750 and 850 nm for their TSS prediction model. In the current study, the model developed for Chardonnay incorporated three of

these same bands (within the ± 20 nm range) out of the seven bands available for inclusion in the models for this study. This suggests that there may be consistent spectral signature changes at these predefined wavelengths for Chardonnay, which could serve as reliable indicators of TSS. However, the models for Cabernet Franc and Riesling did not include these same bands, implying that varietal differences influence the spectral response. Thus, suggesting TSS prediction models need to be tailored to each grape variety, with spectral relationships requiring individual evaluation and validation. It is also worth noting that most studies do not specify exact band lengths utilized in their models but instead provide ranges, making it difficult to draw direct comparisons with the bands used in the presented Cabernet Franc and Riesling models.

### 4.3.2 Factors Contributing to Model Performance and Prediction Accuracy

The predictive performance of the models in this study was lower than that reported in several other studies. For instance, Fernández-Novales et al. (2019a) demonstrated a highly accurate variation of a PLS model used to predict TSS (10.7 - 25.2 °Brix) in Grenache grapes (a red variety) using spectrometry in the 570–998 nm range, achieving an $R^2$ value of 0.95. Similarly, Ebrahimi et al. (2024) explored various spectrometry methods to develop PLS models for TSS prediction, with models for French Colombard (a white variety; TSS range 10.9 - 24.8 °Brix) and Cabernet Sauvignon (a red variety; TSS range 7.0 - 25.5 °Brix) showing $R^2$ values of 0.79 and 0.85, respectively. In contrast, Santos-Campos et al. (2023) applied a range of modeling techniques using spectrometry in the 340–850 nm range to predict TSS (~10 – 25 °Brix; TSS values not included in the paper), and although their PLS model showed moderate accuracy, it only achieved an $R^2$ value of 0.63.

The lower-than-expected performance of the models could be attributed to the limited spectral bands used in the analysis. The models developed in this study focused on identifying TSS relationships within the 610-860 nm range. While there are several important wavelengths within this range for predicting TSS, many of the other models reported in the literature incorporate wavelengths above 860 nm. For example, Benelli et al. (2021) developed a TSS prediction model using spectral data in the 400-1000 nm range for Sangiovese grapes (a red variety). The VIP analysis of this model suggests that spectral data below 700 nm is not crucial, while data above 700 nm is highly informative (Benelli et al., 2021). As discussed above, Ebrahimi et al. (2024) developed models for French Colombard and Cabernet Sauvignon grapes with high accuracy. An additional finding from their study indicated that their original spectral range of 350-2500 nm was too broad and could be reduced to 400-1300 nm while maintaining accuracy. Further, work by Golic et al. (2003) suggests that spectra around 910, 1100, and 1200 nm are particularly useful for detecting CH groups in sugars, and therefore band lengths above 900 nm can be useful in the predication and monitoring of TSS of grapes.

This study was limited by the number of spectral bands available for model development, as the TTWs provide a restricted range of bands. However, the inclusion of additional spectral bands in future iterations of the TTWs could be explored to enhance model performance. Expanding the spectral range may improve predictive accuracy by incorporating supplemental relevant wavelengths in the 900-1000nm that can capture additional chemical changes in grape composition during maturation.

Another potential contributing factor for the lower accuracy of the models in this study is the decision to utilize whole grape clusters rather than individual berries. Most studies on TSS prediction have used single berry measurements for spectrometry readings, which tend to yield more uniform results (Benelli et al., 2021; Trought et al., 2017). However, whole grape clusters were employed in this study to align with the design and intent of the TTW system for continuous TSS monitoring throughout the growing season in the vineyard.

A challenge of using whole clusters is the increased intra-bunch berry variation in TSS, especially when grapes are immature and have low TSS levels (Trought et al., 2017; Wolpert et al., 1980). Although the sensor placement was consistent in this study, with the grape clusters touching the TTW and the rachis orientated upwards, the inherent TSS variation within developing grape clusters may have affected the must sample, leading to discrepancies in TSS readings relative to the measured spectral signature.

For instance, Tang et al. (2019) improved model accuracy by excluding readings below 16 °Brix when modeling whole cluster TSS with spectrometry. However, this approach could not be applied in the current study due to the insufficient data for models based solely on TSS values above 16 °Brix. However, since Cabernet Franc matured later thus, resulting in more data in higher °Brix level range to use in the model, therefore, potentially contributing to the more consistent relationships and to a better-fitting model.

Lastly, regarding model performance, another potential factor contributing to the higher performance of the Cabernet Franc model could be the influence of cultivation style. Cabernet Franc at ON_VIN_03 is produced organically, and as such, the grape skins may lack residues

commonly found on the Riesling and Chardonnay grapes due to the absence of spray application. Although studies are limited to the direct influence of chemical residue on NIR model estimation for TSS, research indicates that NIR analysis via hyperspectral imaging can detect pesticide residues on grapes (Ye et al., 2022). Therefore, the spectra from Cabernet Franc grapes may exhibit fewer interfering signals or less noise associated with chemical residues, which could improve the model's performance.

However, Larrain et al. (2008) found that dust did not influence the performance of NIR spectroscopy in estimating TSS in grapes. Similarly, Urrasa et al. (2016) reported that the presence of epicuticular wax, a naturally occurring wax on grape skins, did not result in a statistically significant difference in model performance for predicting TSS. Therefore, leading to uncertainty about the exact influence that organic cultivation may have had on model performance. As such, more comprehensive studies are required to better understand the role of spray residues, which would also inform the transferability of models across different vineyards and management practices.

### 4.3.3 Exploring the Potential of TTWs for Monitoring Additional Maturity Parameters

Several studies have demonstrated that NIR analysis can effectively model and predict anthocyanin concentrations, another key indicator of grape maturity in red grape varieties, using methods similar to those employed for measuring TSS (Fadock et al., 2016; Fernández-Novales et al., 2019b). Anthocyanins are polyphenolic compounds responsible for the red pigmentation in grape skins (Fernández-Novales et al., 2019b). As Cabernet Franc is a red grape variety, anthocyanins are present in the fruit, in contrast to white grape varieties such as Chardonnay and

Riesling, where anthocyanins are either absent or present in very low concentrations. Since Chardonnay and Riesling do not exhibit the same anthocyanin concentrations, this may help explain the lower $R^2$ values observed for these white grape models. In contrast, the higher accuracy of the Cabernet Franc models could be attributed to the presence of anthocyanins in the grape berries.

Fadock et al. (2016) demonstrated that anthocyanin concentration in Cabernet Franc, along with other red-skinned grape varieties, can be effectively modeled using a PLS model with spectroscopy in the range of 190–852 nm. Similarly, Fernández-Novales et al. (2019b) showed that anthocyanin concentration in red-skinned grapes can be modeled using spectroscopy within the 570–900 nm range. Both of these light ranges align with those used in our models (Fadock et al., 2016; Fernández-Novales et al., 2019b), suggesting that the Cabernet Franc model in this study may also be detecting variations in anthocyanin concentration. Since anthocyanin levels increase alongside TSS during berry maturation, it is plausible that anthocyanin concentration contributes to the higher accuracy of the Cabernet Franc model (Gutiérrez et al., 2019). This suggests an additional application for TTWs: the monitoring of anthocyanin concentrations in red grape varieties through the development of specialized models focused on anthocyanin-spectra relationships.

# Chapter 5: Conclusion

Changing weather patterns associated with climate change are significantly impacting grapevine health, affecting both the quality of the fruit and the resulting wine. To address these challenges, innovative approaches are required to enhance vine health monitoring. One such approach involves exploring transmitted light-based VIs using TTWs, which can provide continuous, detailed measurements to give insight into vine health and fruit maturity.

This research demonstrates that TTW sensors can be effectively deployed in a commercial vineyard setting for continuous monitoring of vine health. $NDVI_T$ values measured using TTWs throughout the growing season followed expected trends, remaining within normal ranges, and were responsive to canopy changes caused by weather events. These findings validate the first two objectives of this study: i) TTW sensors can be used in commercial vineyards to gain valuable insights into vine health; ii) NDVI can be calculated using light transmitted through the canopy. Additionally, it was found that $NDVI_T$ is sensitive to atmospheric conditions, such as $T_A$ and precipitation, indicating that the $NDVI_T$ has the potential to help navigate viticulturists through changing climate.

Regarding the use of TTWs for monitoring grape cluster maturity, this study establishes that the optimal distance between the fruit and the TTW sensor is direct contact between the berries and the sensor; otherwise, oversaturation of the values may occur. The current study suggests that each grape variety may have its own unique relationship between spectral interactions and fruit maturity. However, the 680 nm band, which relates to chlorophyll content, was important in all models. The predictive capabilities of the models showed mixed results, with the Cabernet Franc

model outperforming the others. The model predicting TSS in Cabernet Franc was able to explain 59% of the variance ($R^2 = 0.59$) and yielded a moderate prediction error (RMSEP = 4.12). Overall, in answer to objective (iii) TTW sensors have the potential to serve as an alternative to traditional destructive methods for measuring TSS in viticulture. However, further refinement of the relationships between the NIR spectral bands collected by TTW sensors is necessary to develop robust and highly accurate models for TSS in both red and white grape varieties. TSS models created for spectral analysis with the transmitted light measured by TTW sensors show promise to provide vintners with reliable tools to navigate grape and wine production amidst the challenges posed by a changing climate.

## 5.1 Project limitations and suggestions for future research

This study identified two major limitations in the use of TTWs for monitoring vine health. First, the research focused exclusively on Cabernet Franc vine health in two vineyards. To better understand the relationships between $NDVI_T$ and vine health, future studies should include a broader range of grape varieties. By expanding the variety of vines, it will be determined if $NDVI_T$ can be a universal indicator of vine health like NDVI, or if varietal differences are present. Second, the study deployed only four TTWs within a single row of each of the vineyards, limiting the ability of the current study to determine if TTWs can identify spatial variability across the vineyard. Future research should investigate how TTWs can capture spatial variability across larger vineyard by deploying TTWs throughout variety blocks to enhance the utility of TTWs as a tool for viticulturists monitoring vine health across the vineyard environments.

Additionally, the vine health monitoring portion of this study focused solely on NDVI. However, other VIs, such as the Normalized Difference Greenness Vegetation Index (NDGVI) and Transformed Chlorophyll Absorption in Reflectance Index (TCARI) may provide additional insights into different vine health parameters, offering a broader view of vineyard conditions. For example, NDGVI has the potential to give insight into the nitrogen up take of the vines (Ye et al., 2022), while TCARI can give alternative perspectives of chlorophyll content of the vines (Haboudane et al., 2002).

The investigation into using TTWs to monitor grape maturity was limited by the sample size for each model. Specifically, the earlier harvest times of Chardonnay and Riesling restricted the number of samples with higher TSS concentrations that could be collected. In future studies, more frequent or larger sample sizes from these varieties after verasion would likely enhance the robustness of the models. Furthermore, the models were limited to the wave lengths on the first iteration for the TTWs that were modified from TTs, which are optimized to monitor forest vegetation. To further support the TTWs in monitoring grape maturity, the inclusion of wavelengths in the 900–1000 nm range in the TTWs should be considered, as they may improve the accuracy of grape maturity predictions. Once strong relationships between the spectra and TSS are established, future studies can explore the transferability of these relationships to a vineyard setting, aiming to create a practical tool for viticulturists.

The current study also demonstrated that TTWs could be useful for detecting changes in anthocyanin concentrations, as evidenced by the strong results from the Cabernet Franc model. Future research should explore the relationships between the wavelengths used in this study and

anthocyanin concentrations in red grapes to further support viticulturists in monitoring grape maturity and determining optimal harvest times.

## 5.2 Significance of research

Climate change is significantly affecting wine-producing regions, with potential implications for wine quality due to the influence of extreme weather events and shifting climatic conditions on grapevine growth and development. As climate variability intensifies, it is essential for viticulturists to adopt more precise and efficient monitoring methods to maintain high-quality grape production. Traditional vineyard monitoring techniques are often unable to address the complexities of modern viticulture under changing climate conditions. The aim of the study was to explore novel methodologies for monitoring vine health and grape maturity.

The present research leveraged transmitted light-based NDVI to provide vine-specific health data with a higher degree of precision than conventional satellite-derived measurements. The ability to capture continuous, vine-level information enables more accurate, timely responses to changing vineyard conditions, supports the implementation of targeted management interventions, and ultimately has the potential to help facilitate the optimization of vineyard performance while preserving fruit quality. Additionally, the study suggests that TTWs have the potential to serve as a non-destructive alternative to traditional methods of quantifying TSS in grapes, helping to determine optimal harvest times, which can be highly variable due to changing climate conditions. Overall, this research contributes new methods of vine and fruit monitoring to the knowledge base to help viticulturists navigate the challenges of grape and wine production in the context of a rapidly changing climate.

## References


Ammoniaci, M., Kartsiotis, S.-P., Perria, R., Storchi, P., 2021. State of the Art of Monitoring Technologies and Data Processing for Precision Viticulture. Agriculture 11, 201. https://doi.org/10.3390/agriculture11030201

Aronoff, S., 1950. The Absorption Spectra of Chlorophyll and Related Compounds. Chem. Rev. 47, 175–195. https://doi.org/10.1021/cr60147a001

Benelli, A., Cevoli, C., Ragni, L., Fabbri, A., 2021. In-field and non-destructive monitoring of grapes maturity by hyperspectral imaging. Biosystems Engineering 207, 59–67. https://doi.org/10.1016/j.biosystemseng.2021.04.006

Chandrasekaran, I., Panigrahi, S.S., Ravikanth, L., Singh, C.B., 2019. Potential of Near-Infrared (NIR) Spectroscopy and Hyperspectral Imaging for Quality and Safety Assessment of Fruits: an Overview. Food Anal. Methods 12, 2438–2458. https://doi.org/10.1007/s12161-019-01609-1

Chowdhury, M., Anand, R., Dhar, T., Kurmi, R., Sahni, R.K., Kushwah, A., 2024. Digital Insights into Plant Health: Exploring Vegetation Indices Through Computer Vision, in: Chouhan, S.S., Singh, U.P., Jain, S. (Eds.), Applications of Computer Vision and Drone Technology in Agriculture 4.0. Springer Nature, Singapore, pp. 7–30. https://doi.org/10.1007/978-981-99-8684-2_2

Conde, C., Silva, P., Fontes, N., Dias, A.C., Tavares, R.M., Sousa, M.J., Agasse, A., Delrot, S., Gerós, H., 2007. Biochemical changes throughout grape berry development and fruit and wine quality. Food 1, 1–22.

Dambergs, R., Gishen, M., Cozzolino, D., 2015. A Review of the State of the Art, Limitations, and Perspectives of Infrared Spectroscopy for the Analysis of Wine Grapes, Must, and Grapevine Tissue. Applied Spectroscopy Reviews 50, 261–278. https://doi.org/10.1080/05704928.2014.966380

Delpierre, N., Dufrêne, E., Soudani, K., Ulrich, E., Cecchini, S., Boé, J., François, C., 2009. Modelling interannual and spatial variability of leaf senescence for three deciduous tree species in France. Agricultural and Forest Meteorology 149, 938–948. https://doi.org/10.1016/j.agrformet.2008.11.014

Diago, M.P., Tardaguila, J., Barrio, I., Fernández-Novales, J., 2022. Combination of multispectral imagery, environmental data and thermography for on-the-go monitoring of the grapevine water status in commercial vineyards. European Journal of Agronomy 140, 126586. https://doi.org/10.1016/j.eja.2022.126586

Droulia, F., Charalampopoulos, I., 2021. Future Climate Change Impacts on European Viticulture: A Review on Recent Scientific Advances. Atmosphere 12, 495. https://doi.org/10.3390/atmos12040495

Ebrahimi, I., de Castro, R., Ehsani, R., Brillante, L., Feng, S., 2024. Advancing grape chemical analysis through machine learning and multi-sensor spectroscopy. Journal of Agriculture and Food Research 16, 101085. https://doi.org/10.1016/j.jafr.2024.101085

Environment and Climate Change Canada, 2024. Canadian Climate Normals 1991-2020 Data: Vineland.

Environment and Climate Change, 2023. Climate data: Daily data for station ID 31367, Ontario.

Espinoza, C.Z., Khot, L.R., Sankaran, S., Jacoby, P.W., 2017. High Resolution Multispectral and Thermal Remote Sensing-Based Water Stress Assessment in Subsurface Irrigated Grapevines. Remote Sensing 9, 961. https://doi.org/10.3390/rs9090961

Esteban, M.A., Villanueva, M.J., Lissarrague, J.R., 2002. Relationships between different berry components in Tempranillo (Vitis vinifera L) grapes from irrigated and non-irrigated vines during ripening. Journal of the Science of Food and Agriculture 82, 1136–1146. https://doi.org/10.1002/jsfa.1149

Fadock, M., Brown, R.B., Reynolds, A.G., 2016. Visible-Near Infrared Reflectance Spectroscopy for Nondestructive Analysis of Red Wine Grapes. Am J Enol Vitic. 67, 38–46. https://doi.org/10.5344/ajev.2015.15035

Fernández-Novales, J., Garde-Cerdán, T., Tardáguila, J., Gutiérrez-Gamboa, G., Pérez-Álvarez, E.P., Diago, M.P., 2019a. Assessment of amino acids and total soluble solids in intact grape berries using contactless Vis and NIR spectroscopy during ripening. Talanta 199, 244–253. https://doi.org/10.1016/j.talanta.2019.02.037

Fernández-Novales, J., Tardáguila, J., Gutiérrez, S., Diago, M.P., 2019b. On-The-Go VIS + SW − NIR Spectroscopy as a Reliable Monitoring Tool for Grape Composition within the Vineyard. Molecules 24, 2795. https://doi.org/10.3390/molecules24152795

Ferrara, G., Marcotuli, V., Didonna, A., Stellacci, A.M., Palasciano, M., Mazzeo, A., 2022a. Ripeness Prediction in Table Grape Cultivars by Using a Portable NIR Device. Horticulturae 8, 613. https://doi.org/10.3390/horticulturae8070613

Ferrara, G., Melle, A., Marcotuli, V., Botturi, D., Fawole, O.A., Mazzeo, A., 2022b. The prediction of ripening parameters in Primitivo wine grape cultivar using a portable NIR device. Journal of Food Composition and Analysis 114, 104836. https://doi.org/10.1016/j.jfca.2022.104836

Fraga, H., 2019. Viticulture and Winemaking under Climate Change. Agronomy-Basel 9, 783. https://doi.org/10.3390/agronomy9120783

Fredes, S.N., Ruiz, L.Á., Recio, J.A., 2021. Modeling °Brix and pH in Wine Grapes from Satellite Images in Colchagua Valley, Chile. Agriculture 11, 697. https://doi.org/10.3390/agriculture11080697

Freeman, B.M., Cullis, B.R., 1981. Effect of Hedge Shape for Mechanical Pruning of Vinifera Vines. Am J Enol Vitic. 32, 21–25. https://doi.org/10.5344/ajev.1981.32.1.21

Fuentes, S., Poblete-Echeverría, C., Ortega-Farias, S., Tyerman, S., De Bei, R., 2014. Automated estimation of leaf area index from grapevine canopies using cover photography, video and computational analysis methods. Australian Journal of Grape and Wine Research 20, 465–473. https://doi.org/10.1111/ajgw.12098

Fund, C.C.A., Bootsma, A., Castonguay, Y., Mongrain, D., 2001. Impact of climate change on risk of winter damage to agricultural perennial plants [Impact des changements climatiques sur les risques de dommages hivernaux aux plantes agricoles pérennes].

Gambetta, G.A., Kurtural, S.K., 2021. Global warming and wine quality: are we close to the tipping point? OENO One 55, 353–361. https://doi.org/10.20870/oeno-one.2021.55.3.4774

Gatti, M., Dosso, P., Maurino, M., Merli, M.C., Bernizzoni, F., José Pirez, F., Platè, B., Bertuzzi, G.C., Poni, S., 2016. MECS-VINE®: A New Proximal Sensor for Segmented Mapping of Vigor and Yield Parameters on Vineyard Rows. Sensors 16, 2009. https://doi.org/10.3390/s16122009

Gatti, M., Garavani, A., Squeri, C., Diti, I., De Monte, A., Scotti, C., Poni, S., 2022. Effects of intra-vineyard variability and soil heterogeneity on vine performance, dry matter and nutrient partitioning. Precision Agric 23, 150–177. https://doi.org/10.1007/s11119-021-09831-w

Gatti, M., Garavani, A., Vercesi, A., Poni, S., 2017. Ground-truthing of remotely sensed within-field variability in a cv. Barbera plot for improving vineyard management. Australian Journal of Grape and Wine Research 23, 399–408. https://doi.org/10.1111/ajgw.12286

Gessler, C., Pertot, I., Perazzolli, M., 2011. Plasmopara viticola: a review of knowledge on downy mildew of grapevine and effective disease management. Phytopathologia Mediterranea 50, 3–44. https://doi.org/10.14601/Phytopathol_Mediterr-9360

Giovanelli, G., Brenna, O.V., 2007. Evolution of some phenolic components, carotenoids and chlorophylls during ripening of three Italian grape varieties. Eur Food Res Technol 225, 145–150. https://doi.org/10.1007/s00217-006-0436-4

Giovenzana, V., Beghi, R., Malegori, C., Civelli, R., Guidetti, R., 2014. Wavelength Selection with a View to a Simplified Handheld Optical System to Estimate Grape Ripeness. Am J Enol Vitic. 65, 117–123. https://doi.org/10.5344/ajev.2013.13024

Giovenzana, V., Civelli, R., Beghi, R., Oberti, R., Guidetti, R., 2015. Testing of a simplified LED based vis/NIR system for rapid ripeness evaluation of white grape (*Vitis vinifera* L.) for *Franciacorta* wine. Talanta 144, 584–591. https://doi.org/10.1016/j.talanta.2015.06.055

Giovos, R., Tassopoulos, D., Kalivas, D., Lougkos, N., Priovolou, A., 2021. Remote Sensing Vegetation Indices in Viticulture: A Critical Review. Agriculture 11, 457. https://doi.org/10.3390/agriculture11050457

Golic, M., Walsh, K., Lawson, P., 2003. Short-Wavelength Near-Infrared Spectra of Sucrose, Glucose, and Fructose with Respect to Sugar Concentration and Temperature. Appl Spectrosc 57, 139–145. https://doi.org/10.1366/000370203321535033

Gomes, V.M., Fernandes, A.M., Faia, A., Melo-Pinto, P., 2017. Comparison of different approaches for the prediction of sugar content in new vintages of whole Port wine grape berries using hyperspectral imaging. Computers and Electronics in Agriculture 140, 244–254. https://doi.org/10.1016/j.compag.2017.06.009

Gorelick, N., Hancher, M., Dixon, M., Ilyushchenko, S., Thau, D., Moore, R., 2017. Google Earth Engine: Planetary-scale geospatial analysis for everyone. Remote Sensing of Environment, Big Remotely Sensed Data: tools, applications and experiences 202, 18–27. https://doi.org/10.1016/j.rse.2017.06.031

Guo, Y., Ren, G., Zhang, K., Li, Z., Miao, Y., Guo, H., 2021. Leaf senescence: progression, regulation, and application. Mol Horticulture 1, 5. https://doi.org/10.1186/s43897-021-00006-9

Gutiérrez, S., Tardaguila, J., Fernández-Novales, J., Diago, M. p., 2019. On-the-go hyperspectral imaging for the in-field estimation of grape berry soluble solids and anthocyanin concentration. Australian Journal of Grape and Wine Research 25, 127–133. https://doi.org/10.1111/ajgw.12376

Gutiérrez-Gamboa, G., Zheng, W., Martínez de Toda, F., 2021. Current viticultural techniques to mitigate the effects of global warming on grape and wine quality: A comprehensive review. Food Research International 139, 109946. https://doi.org/10.1016/j.foodres.2020.109946

Haboudane, D., Miller, J.R., Tremblay, N., Zarco-Tejada, P.J., Dextraze, L., 2002. Integrated narrow-band vegetation indices for prediction of crop chlorophyll content for application to precision agriculture. Remote Sensing of Environment 81, 416–426. https://doi.org/10.1016/S0034-4257(02)00018-4

Hall, A., Lamb, D. w., Holzapfel, B., Louis, J., 2002. Optical remote sensing applications in viticulture - a review. Australian Journal of Grape and Wine Research 8, 36–47. https://doi.org/10.1111/j.1755-0238.2002.tb00209.x

Herrera, J., Guesalaga, A., Agosin, E., 2003. Shortwave–near infrared spectroscopy for non-destructive determination of maturity of wine grapes. Meas. Sci. Technol. 14, 689. https://doi.org/10.1088/0957-0233/14/5/320

Hewer, M.J., Brunette, M., 2020. Climate change impact assessment on grape and wine for Ontario, Canada's appellations of origin. Reg Environ Change 20, 86. https://doi.org/10.1007/s10113-020-01673-y

Jackson, D.I., Lombard, P.B., 1993. Environmental and Management Practices Affecting Grape Composition and Wine Quality - A Review. Am J Enol Vitic. 44, 409–430. https://doi.org/10.5344/ajev.1993.44.4.409

Jia, K., Hasan, U., Jiang, H., Qin, B., Chen, S., Li, D., Wang, C., Deng, Y., Shen, J., 2024. How frequent the Landsat 8/9-Sentinel 2A/B virtual constellation observed the earth for continuous time series monitoring. International Journal of Applied Earth Observation and Geoinformation 130, 103899. https://doi.org/10.1016/j.jag.2024.103899

Johnson, L.F., 2003. Temporal stability of an NDVI-LAI relationship in a Napa Valley vineyard. Australian Journal of Grape and Wine Research 9, 96–101. https://doi.org/10.1111/j.1755-0238.2003.tb00258.x

Johnson, L.F., Roczen, D., Youkhana, S., 2001. Vineyard canopy density mapping with IKONOS satellite imagery. Presented at the Proceedings of the Third International Conference on Geospatial Information in Agriculture and Forestry, Denver, CO, USA, pp. 5–7.

Johnson, L.F., Roczen, D.E., Youkhana, S.K., Nemani, R.R., Bosch, D.F., 2003. Mapping vineyard leaf area with multispectral satellite imagery. Computers and Electronics in Agriculture 38, 33–44. https://doi.org/10.1016/S0168-1699(02)00106-0

Jordão, A.M., Vilela, A., Cosme, F., 2015. From Sugar of Grape to Alcohol of Wine: Sensorial Impact of Alcohol in Wine. Beverages 1, 292–310. https://doi.org/10.3390/beverages1040292

Kasimati, A., Espejo-García, B., Darra, N., Fountas, S., 2022. Predicting Grape Sugar Content under Quality Attributes Using Normalized Difference Vegetation Index Data and Automated Machine Learning. Sensors 22, 3249. https://doi.org/10.3390/s22093249

Kasimati, A., Espejo-Garcia, B., Vali, E., Malounas, I., Fountas, S., 2021. Investigating a Selection of Methods for the Prediction of Total Soluble Solids Among Wine Grape Quality Characteristics

Using Normalized Difference Vegetation Index Data From Proximal and Remote Sensing. Frontiers in Plant Science 12. https://doi.org/10.3389/fpls.2021.683078

Kazmierski, M., Glémas, P., Rousseau, J., Tisseyre, B., 2011. Temporal stability of within-field patterns of NDVI in non irrigated Mediterranean vineyards. OENO One 45, 61–73. https://doi.org/10.20870/oeno-one.2011.45.2.1488

Khaliq, A., Comba, L., Biglia, A., Ricauda Aimonino, D., Chiaberge, M., Gay, P., 2019. Comparison of Satellite and UAV-Based Multispectral Imagery for Vineyard Variability Assessment. Remote Sensing 11, 436. https://doi.org/10.3390/rs11040436

Khodabakhshian, R., Emadi, B., Khojastehpour, M., Golzarian, M.R., Sazgarnia, A., 2017. Non-destructive evaluation of maturity and quality parameters of pomegranate fruit by visible/near infrared spectroscopy. International Journal of Food Properties 20, 41–52. https://doi.org/10.1080/10942912.2015.1126725

Knipling, E.B., 1970. Physical and physiological basis for the reflectance of visible and near-infrared radiation from vegetation. Remote Sensing of Environment 1, 155–159.

Kotsaki, E., Reynolds, A.G., Brown, R., Jollineau, M., Lee, H.-S., Aubie, E., 2020a. Proximal Sensing and Relationships to Soil and Vine Water Status, Yield, and Berry Composition in Ontario Vineyards. Am J Enol Vitic. 71, 114–131. https://doi.org/10.5344/ajev.2019.19018

Kotsaki, E., Reynolds, A.G., Brown, R., Lee, H.-S., Jollineau, M., 2020b. Spatial Variability in Soil and Vine Water Status in Ontario Vineyards: Relationships to Yield and Berry Composition. Am J Enol Vitic. 71, 132–148. https://doi.org/10.5344/ajev.2019.19019

Larrain, M., Guesalaga, A.R., Agosin, E., 2008. A Multipurpose Portable Instrument for Determining Ripeness in Wine Grapes Using NIR Spectroscopy. IEEE Transactions on Instrumentation and Measurement 57, 294–302. https://doi.org/10.1109/TIM.2007.910098

Lee, J.C., Bruck, D.J., Dreves, A.J., Ioriatti, C., Vogt, H., Baufeld, P., 2011. In Focus: Spotted wing drosophila, Drosophila suzukii, across perspectives. Pest Management Science 67, 1349–1351. https://doi.org/10.1002/ps.2271

Li, Z., Zhao, T., Liu, J., Li, H., Liu, B., 2023. Shade-Induced Leaf Senescence in Plants. Plants 12, 1550. https://doi.org/10.3390/plants12071550

Lieth, H., 1973. Primary production: Terrestrial ecosystems. Hum Ecol 1, 303–332. https://doi.org/10.1007/BF01536729

Liew, O.W., Chong, P.C.J., Li, B., Asundi, A.K., 2008. Signature Optical Cues: Emerging Technologies for Monitoring Plant Health. Sensors 8, 3205–3239. https://doi.org/10.3390/s8053205

Liland, K.H., Mevik, B.-H., Wehrens, R., 2023. pls: Partial Least Squares and Principal Component Regression.

Marchesini, L.B., Cavagna, M., Chini, I., Gianelle, D., Vescovo, L., Zampedri, R., 2023. Radiometric calibration of the TreeTalker (TT+) spectrometer. Zenodo. https://doi.org/10.5281/zenodo.10050189

Matese, A., Di Gennaro, S.F., 2021. Beyond the traditional NDVI index as a key factor to mainstream the use of UAV in precision viticulture. Sci Rep 11, 2721. https://doi.org/10.1038/s41598-021-81652-3

Matese, A., Di Gennaro, S.F., Orlandi, G., Gatti, M., Poni, S., 2022. Assessing Grapevine Biophysical Parameters From Unmanned Aerial Vehicles Hyperspectral Imagery. Frontiers in Plant Science 13.

Matese, A., Gennaro, S.F.D., 2015. Technology in precision viticulture: a state of the art review. IJWR 7, 69–81. https://doi.org/10.2147/IJWR.S69405

McGlone, V.A., Kawano, S., 1998. Firmness, dry-matter and soluble-solids assessment of postharvest kiwifruit by NIR spectroscopy. Postharvest Biology and Technology 13, 131–141. https://doi.org/10.1016/S0925-5214(98)00007-6

Molitor, D., Junk, J., 2019. Climate change is implicating a two-fold impact on air temperature increase in the ripening period under the conditions of the Luxembourgish grapegrowing region. OENO One 53. https://doi.org/10.20870/oeno-one.2019.53.3.2329

Mucalo, A., Matić, D., Morić-Špranić, A., Čagalj, M., 2024. Satellite Solutions for Precision Viticulture: Enhancing Sustainability and Efficiency in Vineyard Management. Agronomy 14, 1862. https://doi.org/10.3390/agronomy14081862

Nicolaï, B.M., Beullens, K., Bobelyn, E., Peirs, A., Saeys, W., Theron, K.I., Lammertyn, J., 2007. Nondestructive measurement of fruit and vegetable quality by means of NIR spectroscopy: A review. Postharvest Biology and Technology 46, 99–118. https://doi.org/10.1016/j.postharvbio.2007.06.024

Ojeda, H., Deloire, A., Carbonneau, A., 2001. Influence of water deficits on grape berry growth. VITIS-GEILWEILERHOF- 40, 141–146.

Oliveira, H.M., Tugnolo, A., Fontes, N., Marques, C., Geraldes, Á., Jenne, S., Zappe, H., Graça, A., Giovenzana, V., Beghi, R., Guidetti, R., Piteira, J., Freitas, P., 2024. An autonomous Internet of Things spectral sensing system for in-situ optical monitoring of grape ripening: design, characterization, and operation. Computers and Electronics in Agriculture 217, 108599. https://doi.org/10.1016/j.compag.2023.108599

OMAFRA GIS, 2019. Soil Survey Complex.

Padua, L., Marques, P., Adao, T., Guimaraes, N., Sousa, A., Peres, E., Sousa, J.J., 2019. Vineyard Variability Analysis through UAV-Based Vigour Maps to Assess Climate Change Impacts. Agronomy-Basel 9, 581. https://doi.org/10.3390/agronomy9100581

Pampuri, A., Tugnolo, A., Giovenzana, V., Casson, A., Pozzoli, C., Brancadoro, L., Guidetti, R., Beghi, R., 2022. Application of a Cost-Effective Visible/Near Infrared Optical Prototype for the Measurement of Qualitative Parameters of Chardonnay Grapes. Applied Sciences 12, 4853. https://doi.org/10.3390/app12104853

Pickering, K., Plummer, R., Shaw, T., Pickering, G., 2015a. Assessing the adaptive capacity of the Ontario wine industry for climate change adaptation. International Journal of Wine Research 15, 13–27.

Pickering, K., Plummer, R., Shaw, T., Pickering, G., 2015b. Assessing the adaptive capacity of the Ontario wine industry for climate change adaptation. International Journal of Wine Research 15, 13–27.

Pons, A., Allamy, L., Schüttler, A., Rauhut, D., Thibon, C., Darriet, P., 2017. What is the expected impact of climate change on wine aroma compounds and their precursors in grape? OENO One 51, 141–146. https://doi.org/10.20870/oeno-one.2017.51.2.1868

Pour, A.B., Ranjbar, H., Sekandari, M., Abd El-Wahed, M., Hossain, M.S., Hashim, M., Yousefi, M., Zoheir, B., Wambo, J.D.T., Muslim, A.M., 2023. 2 - Remote sensing for mineral exploration, in: Pour, A.B., Parsa, M., Eldosouky, A.M. (Eds.), Geospatial Analysis Applied to Mineral Exploration. Elsevier, pp. 17–149. https://doi.org/10.1016/B978-0-323-95608-6.00002-0

Pu, H., Liu, D., Wang, L., Sun, D.-W., 2016. Soluble Solids Content and pH Prediction and Maturity Discrimination of Lychee Fruits Using Visible and Near Infrared Hyperspectral Imaging. Food Anal. Methods 9, 235–244. https://doi.org/10.1007/s12161-015-0186-7

R Core Team, 2021. R: A Language and Environment for Statistical Computing.

Reynolds, A.G., Lee, H.-S., Dorin, B., Brown, R., Jollineau, M., Shemrock, A., Crombleholme, M., Poirier, E.J., Zheng, W., Gasnier, M., Shabanian, M., Meng, B., 2018. Mapping Cabernet Franc

vineyards by unmanned aerial vehicles (UAVs) for variability in vegetation indices, water status, and virus titer. E3S Web Conf. 50, 02010. https://doi.org/10.1051/e3sconf/20185002010

Rienth, M., Vigneron, N., Walker, R.P., Castellarin, S.D., Sweetman, C., Burbidge, C.A., Bonghi, C., Famiani, F., Darriet, P., 2021. Modifications of Grapevine Berry Composition Induced by Main Viral and Fungal Pathogens in a Climate Change Scenario. Front. Plant Sci. 12. https://doi.org/10.3389/fpls.2021.717223

Robinson, S.P., Davies, C., 2000. Molecular biology of grape berry ripening. Australian Journal of Grape and Wine Research 6, 175–188. https://doi.org/10.1111/j.1755-0238.2000.tb00177.x

Romero, M., Luo, Y., Su, B., Fuentes, S., 2018. Vineyard water status estimation using multispectral imagery from an UAV platform and machine learning algorithms for irrigation scheduling management. Computers and Electronics in Agriculture 147, 109–117. https://doi.org/10.1016/j.compag.2018.02.013

Rous, J.W., Haas, R.H., Schell, J.A., Deering, D.W., 1973. MONITORING THE VERNAL ADVANCEMENT AND RETROGRADATION (GREEN WAVE EFFECT)OF NATURAL VEGETATION. Texas A&M University, College Station, Texas.

Sadras, V. o., Moran, M. a., 2012. Elevated temperature decouples anthocyanins and sugars in berries of Shiraz and Cabernet Franc. Australian Journal of Grape and Wine Research 18, 115–122. https://doi.org/10.1111/j.1755-0238.2012.00180.x

Santos, J.A., Fraga, H., Malheiro, A.C., Moutinho-Pereira, J., Dinis, L.-T., Correia, C., Moriondo, M., Leolini, L., Dibari, C., Costafreda-Aumedes, S., Kartschall, T., Menz, C., Molitor, D., Junk, J., Beyer, M., Schultz, H.R., 2020. A Review of the Potential Climate Change Impacts and Adaptation Options for European Viticulture. Appl. Sci.-Basel 10, 3092. https://doi.org/10.3390/app10093092

Santos-Campos, M., Tosin, R., Rodrigues, L., Gonçalves, I., Barbosa, C., Martins, R., Santos, F., Cunha, M., 2023. Enhancing Grape Brix Prediction in Precision Viticulture: A Benchmarking Study of Predictive Models Using Hyperspectral Proximal Sensors. Biology and Life Sciences Forum 27, 50. https://doi.org/10.3390/IECAG2023-15914

Serrano, L., González-Flor, C., Gorchs, G., 2012. Assessment of grape yield and composition using the reflectance based Water Index in Mediterranean rainfed vineyards. Remote Sensing of Environment 118, 249–258. https://doi.org/10.1016/j.rse.2011.11.021

Serrano, L., Gorchs, G., 2022. Water Availability Affects the Capability of Reflectance Indices to Estimate Berry Yield and Quality Attributes in Rain-Fed Vineyards. Agronomy 12, 2091. https://doi.org/10.3390/agronomy12092091

Sgubin, G., Swingedouw, D., Dayon, G., García de Cortázar-Atauri, I., Ollat, N., Pagé, C., van Leeuwen, C., 2018. The risk of tardive frost damage in French vineyards in a changing climate. Agricultural and Forest Meteorology 250–251, 226–242. https://doi.org/10.1016/j.agrformet.2017.12.253

Shaw, T.B., 2017. Climate change and the evolution of the Ontario cool climate wine regions in Canada. Journal of Wine Research 28, 13–45. https://doi.org/10.1080/09571264.2016.1238349

Sinton, T.H., Ough, C.S., Kissler, J.J., Kasimatis, A.N., 1978. Grape Juice Indicators for Prediction of Potential Wine Quality. I. Relationship Between Crop Level, Juice and Wine Composition, and Wine Sensory Ratings and Scores. Am J Enol Vitic. 29, 267–271. https://doi.org/10.5344/ajev.1978.29.4.267

Smart, R.E., 1985. Principles of Grapevine Canopy Microclimate Manipulation with Implications for Yield and Quality. A Review. Am J Enol Vitic. 36, 230–239. https://doi.org/10.5344/ajev.1985.36.3.230

Soubry, I., Patias, P., Tsioukas, V., 2017. Monitoring vineyards with UAV and multi-sensors for the assessment of water stress and grape maturity. J. Unmanned Veh. Sys. 5, 37–50. https://doi.org/10.1139/juvs-2016-0024

Squeri, C., Poni, S., Di Gennaro, S.F., Matese, A., Gatti, M., 2021. Comparison and Ground Truthing of Different Remote and Proximal Sensing Platforms to Characterize Variability in a Hedgerow-Trained Vineyard. Remote Sensing 13, 2056. https://doi.org/10.3390/rs13112056

Stamford, J.D., Vialet-Chabrand, S., Cameron, I., Lawson, T., 2023. Development of an accurate low cost NDVI imaging system for assessing plant health. Plant Methods 19, 9. https://doi.org/10.1186/s13007-023-00981-8

Sun, L., Gao, F., Anderson, M.C., Kustas, W.P., Alsina, M.M., Sanchez, L., Sams, B., McKee, L., Dulaney, W., White, W.A., Alfieri, J.G., Prueger, J.H., Melton, F., Post, K., 2017. Daily Mapping of 30 m LAI and NDVI for Grape Yield Prediction in California Vineyards. Remote Sensing 9, 317. https://doi.org/10.3390/rs9040317

Swe, K.N., Takai, S., Noguchi, N., 2023. Novel approaches for a brix prediction model in Rondo wine grapes using a hyperspectral Camera: Comparison between destructive and Non-destructive sensing methods. Computers and Electronics in Agriculture 211, 108037. https://doi.org/10.1016/j.compag.2023.108037

Tang, J., Petrie, P. r., Whitty, M., 2019. Modelling relationships between visible winegrape berries and bunch maturity. Australian Journal of Grape and Wine Research 25, 116–126. https://doi.org/10.1111/ajgw.12374

Tarrio, K., Tang, X., Masek, J.G., Claverie, M., Ju, J., Qiu, S., Zhu, Z., Woodcock, C.E., 2020. Comparison of cloud detection algorithms for Sentinel-2 imagery. Science of Remote Sensing 2, 100010. https://doi.org/10.1016/j.srs.2020.100010

Thimann, K.V., 1985. The interaction of hormonal and environmental factors in leaf senescence. Biol Plant 27, 83–91. https://doi.org/10.1007/BF02902140

Tomelleri, E., Belelli Marchesini, L., Yaroslavtsev, A., Asgharinia, S., Valentini, R., 2022. Toward a Unified TreeTalker Data Curation Process. Forests 13, 855. https://doi.org/10.3390/f13060855

Trought, M.C.T., Naylor, A. p., Frampton, C., 2017. Effect of row orientation, trellis type, shoot and bunch position on the variability of Sauvignon Blanc ( L.) juice composition. Australian Journal of Grape and Wine Research 23, 240–250. https://doi.org/10.1111/ajgw.12275

Urraca, R., Sanz-Garcia, A., Tardaguila, J., Diago, M.P., 2016. Estimation of total soluble solids in grape berries using a hand-held NIR spectrometer under field conditions. Journal of the Science of Food and Agriculture 96, 3007–3016. https://doi.org/10.1002/jsfa.7470

Vaglio Laurin, G., Cotrina-Sanchez, A., Belelli-Marchesini, L., Tomelleri, E., Battipaglia, G., Cocozza, C., Niccoli, F., Kabala, J.P., Gianelle, D., Vescovo, L., Da Ros, L., Valentini, R., 2024. Comparing ground below-canopy and satellite spectral data for an improved and integrated forest phenology monitoring system. Ecological Indicators 158, 111328. https://doi.org/10.1016/j.ecolind.2023.111328

Valentini, R., Belelli Marchesini, L., Gianelle, D., Sala, G., Yarovslavtsev, A., Vasenev, V., Castaldi, S., 2019. New tree monitoring systems: from Industry 4.0 to Nature 4.0. https://doi.org/10.12899/asr-1847

Van Leeuwen, C., Seguin, G., 2006. The concept of terroir in viticulture. Journal of Wine Research 17, 1–10. https://doi.org/10.1080/09571260600633135

van Leeuwen, C., Sgubin, G., Bois, B., Ollat, N., Swingedouw, D., Zito, S., Gambetta, G.A., 2024. Climate change impacts and adaptations of wine production. Nat Rev Earth Environ 5, 258–275. https://doi.org/10.1038/s43017-024-00521-5

Walsh, K.B., Blasco, J., Zude-Sasse, M., Sun, X., 2020. Visible-NIR 'point' spectroscopy in postharvest fruit and vegetable assessment: The science behind three decades of commercial use. Postharvest Biology and Technology 168, 111246. https://doi.org/10.1016/j.postharvbio.2020.111246

Wang, J., Rich, P.M., Price, K.P., 2003. Temporal responses of NDVI to precipitation and temperature in the central Great Plains, USA. International Journal of Remote Sensing 24, 2345–2364. https://doi.org/10.1080/01431160210154812

Wang, W., Paliwal, J., 2007. Near-infrared spectroscopy and imaging in food quality and safety. Sens. & Instrumen. Food Qual. 1, 193–207. https://doi.org/10.1007/s11694-007-9022-0

Wardlow, B.D., Egbert, S.L., Kastens, J.H., 2007. Analysis of time-series MODIS 250 m vegetation index data for crop classification in the U.S. Central Great Plains. Remote Sensing of Environment 108, 290–310. https://doi.org/10.1016/j.rse.2006.11.021

Wickham, H., 2016. ggplot2: Elegant Graphics for Data Analysis.

Wickham, H., François, R., Henry, L., Müller, K., Vaughan, D., 2023. dplyr: A Grammar of Data Manipulation}.

Wolpert, J.A., Howell, G.S., Cress, C.E., 1980. Sampling strategies for estimates of cluster weight, soluble solids and acidity of'Concord'grapes.

Woolley, J.T., 1971. Reflectance and Transmittance of Light by Leaves. Plant Physiology 47, 656–662. https://doi.org/10.1104/pp.47.5.656

Yang, B., Guo, W., Li, W., Li, Q., Liu, D., Zhu, X., 2019. Portable, visual, and nondestructive detector integrating Vis/NIR spectrometer for sugar content of kiwifruits. Journal of Food Process Engineering 42, e12982. https://doi.org/10.1111/jfpe.12982

Yang, W., Yang, L., Merchant, J.W., 1997. An assessment of AVHRR/NDVI-ecoclimatological relations in Nebraska, U.S.A. International Journal of Remote Sensing 18, 2161–2180. https://doi.org/10.1080/014311697217819

Ye, W., Yan, T., Zhang, C., Duan, L., Chen, W., Song, H., Zhang, Y., Xu, W., Gao, P., 2022. Detection of Pesticide Residue Level in Grape Using Hyperspectral Imaging with Machine Learning. Foods 11, 1609. https://doi.org/10.3390/foods11111609

Yu, R., Brillante, L., Martínez-Lüscher, J., Kurtural, S.K., 2020. Spatial Variability of Soil and Plant Water Status and Their Cascading Effects on Grapevine Physiology Are Linked to Berry and Wine Chemistry. Front. Plant Sci. 11. https://doi.org/10.3389/fpls.2020.00790

Zahir, S.A.D.M., Omar, A.F., Jamlos, M.F., Azmi, M.A.M., Muncan, J., 2022. A review of visible and near-infrared (Vis-NIR) spectroscopy application in plant stress detection. Sensors and Actuators A: Physical 338, 113468. https://doi.org/10.1016/j.sna.2022.113468

Zifarelli, A., Giglio, M., Menduni, G., Sampaolo, A., Patimisco, P., Passaro, V.M.N., Wu, H., Dong, L., Spagnolo, V., 2020. Partial Least-Squares Regression as a Tool to Retrieve Gas Concentrations in Mixtures Detected Using Quartz-Enhanced Photoacoustic Spectroscopy. Anal Chem 92, 11035–11043. https://doi.org/10.1021/acs.analchem.0c0007